# A review of the oceanography and Antarctic Bottom Water formation offshore Cape Darnley, East Antarctica

Sienna Neve Blanckensee[1], David E Gwyther[2], Benjamin Keith Galton-Fenzi[3], Kathryn L Gunn[4], Laura Herraiz-Borreguero[5], Kay I. Ohshima[6], Esther Portela Rodriguez[7], Alexandra L Post[8], and Helen Bostock[2]

[1]The University of Queensland
[2]University of Queensland
[3]Australian Antarctic Division
[4]University of Southampton
[5]CSIRO
[6]Institute of Low Temperature Science, Hokkaido University
[7]Univ. Brest, CNRS, IRD, Ifremer, Laboratoire d'Oceanographie Physique et Spatiale (LOPS),
[8]Geoscience Australia

May 02, 2024

**Abstract**

Antarctic Bottom Water (AABW) is the densest water mass in the world and drives the lower limb of the global thermohaline circulation. AABW is formed in only four regions around Antarctica and Cape Darnley, East Antarctica, is the most recently discovered formation region. Here, we compile 40 years of oceanographic data for this region to provide the climatological oceanographic conditions, and review the water mass properties and their role in AABW formation. We split the region into three sectors (East, Central and West) and identified the main water masses, current regimes and their influence on the formation of Cape Darnley Bottom Water (CDBW). In the eastern sector, Prydz Bay, the formation of Ice Shelf Water preconditions the water (cold and fresh) that flows into the central sector to ~68.5*E, enhancing sea ice production in Cape Darnley Polynya. This produces a high salinity variant of DSW (up to 35.15 g/kg) DSW that we coin Burton Basin DSW. In contrast, the western sector of the Cape Darnley Polynya produces a low salinity variant (up to 34.85 g/kg) we coin Nielsen Basin DSW. The resultant combined CDBW is the warmest (upper temperature bound of 0.05*C) AABW formed around Antarctica with an upper bound salinity of ~34.845 g/kg. Our findings will contribute to planning future observing systems at Cape Darnley, determining the role CDBW plays in our global oceanic and climate systems, and modelling past and future climate scenarios.

# A review of the oceanography and Antarctic Bottom Water formation offshore Cape Darnley, East Antarctica

**Sienna N. Blanckensee[1], David E. Gwyther[1], Ben K. Galton-Fenzi [2], Kathryn L. Gunn [3], Laura Herraiz-Borreguero[4],[5], Kay I. Ohshima [6], Esther Portela Rodriguez[7], Alexandra L. Post [8], Helen C. Bostock[1]**

[1]School of the Environment, The University of Queensland, Australia
[2]Australian Antarctic Division, Hobart, Tasmania, Australia
[3]School of Ocean and Earth Science, University of Southampton, Southampton, UK
[4]CSIRO Environment, Hobart, Tas, 7004, Australia
[5]Australian Antarctic Partnership Program, Hobart, Tas, 7004, Australia
[6]Institute of Low Temperature Science, Hokkaido University, Japan
[7]Laboratoire d'Oceanographie Physique et Spatiale (LOPS), University Brest, CNRS, IRD, Ifremer, Plouzane, France
[8]Geoscience Australia, Canberra, Australia

**Key Points:**

- Water masses and processes in Prydz Bay precondition and influence the characteristics of the DSW formation in Cape Darnley to ∼68.5°E
- A high and low salinity variant of DSW is exported from Cape Darnley, observing the highest maximum salinity of all AABW formation sites.
- Cape Darnley Bottom Water has the warmest upper bound temperature of the four sources of AABW.

Corresponding author: Sienna Blanckensee, `s.blanckensee@uq.net.au`

**Abstract**

Antarctic Bottom Water (AABW) is the densest water mass in the world and drives the lower limb of the global thermohaline circulation. AABW is formed in only four regions around Antarctica and Cape Darnley, East Antarctica, is the most recently discovered formation region. Here, we compile 40 years of oceanographic data for this region to provide the climatological oceanographic conditions, and review the water mass properties and their role in AABW formation. We split the region into three sectors (East, Central and West) and identified the main water masses, current regimes and their influence on the formation of Cape Darnley Bottom Water (CDBW). In the eastern sector, Prydz Bay, the formation of Ice Shelf Water preconditions the water (cold and fresh) that flows into the central sector to ∼68.5°E, enhancing sea ice production in Cape Darnley Polynya. This produces a high salinity variant of DSW (up to 35.15 g/kg) DSW that we coin Burton Basin DSW. In contrast, the western sector of the Cape Darnley Polynya produces a low salinity variant (up to 34.85 g/kg) we coin Nielsen Basin DSW. The resultant combined CDBW is the warmest (upper temperature bound of 0.05°C) AABW formed around Antarctica with an upper bound salinity of ∼34.845 g/kg. Our findings will contribute to planning future observing systems at Cape Darnley, determining the role CDBW plays in our global oceanic and climate systems, and modelling past and future climate scenarios.

## Plain Language Summary

Around Antarctica, there are four areas where very high sea ice production makes water dense enough to sink to the sea floor. This water is called Antarctic Bottom Water and plays a vital role in deep water circulation and moving cold water towards the equator, therefore regulating global climate. Cape Darnley, in East Antarctica, is the most recently discovered of these four areas and hence has been less studied. Cape Darnley Bottom Water is unique as it forms via slightly different processes to the other three formation sites. In this study, we have pulled together all the data in the region over a 40-year period for the first time. We found that very cold water flows into the region from upstream, making conditions ideal for very high sea ice production at Cape Darnley. This forms a higher and lower salinity dense water mass that flows down different pathways before combining to become Cape Darnley Bottom Water, which is warmer and saltier than the other three areas. These findings are critical for planning future data collection, understanding the impact this site has on the global ocean circulation, and how climate change could impact Antarctic Bottom Water in the future.

## 1 Introduction

Antarctic Bottom Water (AABW) is the densest water mass in the globe due to its high salinity and cold temperatures. It occupies the abyssal layers of the ocean and accounts for 30-40% of oceanic volume. AABW supplies the lower limb of the meridional overturning circulation (Cougnon et al., 2013; Johnson, 2008) and it plays a key role in the climate system and biogeochemical cycles by transporting cold, salty, oxygen and carbon-rich waters to the deep ocean (Bindoff et al., 2000; Ohshima et al., 2013; Orsi et al., 1999; Shapiro et al., 2003). Over the last 50 years, AABW has experienced freshening, warming, and significant contraction, which threatens this major global circulation (G. D. Williams et al., 2010; Tamura et al., 2008; Fogwill et al., 2015).

AABW forms at four locations around Antarctica: the Weddell Sea, Ross Sea, Adélie Land (Cougnon et al., 2013), and Cape Darnley, most recently discovered in 2013 by Ohshima et al. (2013). Despite a number of studies in the Cape Darnley region (Mizuta et al., 2021; Gao et al., 2022; Aoki et al., 2020; Ohashi et al., 2022; Fraser et al., 2019; Ohshima et al., 2013, 2022) and a growing hydrographic dataset since its discovery, we are yet to determine the mean state of the region and to understand the role each water mass plays in Cape Darnley Bottom Water (CDBW) formation. Here we compile 40 years of oceanographic data to provide an ocean climatology of Cape Darnley for the first time. Our work provides an improved understanding of the characteristics of the Dense Shelf Water (DSW) that forms in the region, which is the precursor to CDBW.

## 2 Oceanographic Context

The DSW mass formed over the continental shelf of Antarctica is the precursor for AABW (Kusahara et al., 2010; Kitade et al., 2014; Ohshima et al., 2013; Cougnon et al., 2013; G. D. Williams et al., 2010). DSW formation requires an active polynya where continuous sea ice production results in brine rejection and significantly increases the density of the water column beneath (Kusahara et al., 2010; Kitade et al., 2014; Ohshima et al., 2013; Cougnon et al., 2013; G. D. Williams et al., 2010). However, the density and formation of DSW is also controlled by other water masses, regional circulation, and shelf geography (Portela et al., 2022).

AABW formation occurs at sites around the Antarctic margin that possess the necessary pre-existing oceanographic conditions and an active polynya. The Ross Sea polynyas exhibit the highest sea ice production (449.2 $km^3$/yr), while the Cape Darnley and Adélie Land polynyas contribute 181 $km^3$/yr and 180 $km^3$/yr respectively, with the Weddell Polynya exhibiting the smallest production rate at 84.6 $km^3$/yr (Tamura et al., 2008; G. D. Williams et al., 2010). However, sea ice production rates are not directly correlated with percentage contribution to global AABW, with the Weddell Sea and Ross Sea contributing 50–60% and 30–40% of the total AABW respectively (Orsi et al., 2002, 1999; Foldvik et al., 2004; Ohshima et al., 2016). The remaining AABW is sourced from East Antarctica, with Cape Darnley contributing 6–13% and Adélie Land contributing 2–9% (Ohshima et al., 2013; Orsi et al., 2002; G. D. Williams et al., 2008).

In the Ross Sea, Weddell Sea and Adélie Land regions, DSW forming polynyas occur over wide and deep coastal embayments, with the polynya typically inland from the continental shelf break (Orsi & Wiederwohl, 2009; Silvano et al., 2020; Foldvik et al., 2004; Wang et al., 2012; Marsland et al., 2004; G. D. Williams et al., 2008). For example, the Ross Sea polynya is 400 km from the shelf break (G. D. Williams et al., 2010). This position and bathymetric conditions play a critical role allowing DSW to accumulate and reach a sufficient density over time, prior to export down the slope to form AABW (G. D. Williams et al., 2016; Foldvik et al., 2004; Ohshima et al., 2016).

DSW formation is also influenced by water masses and ocean circulation north of the continental shelf. The intrusion of warm, salty, offshore Circumpolar Deep Waters (CDW) onto the shelf can also be impacted by slope processes such as the presence of the Antarctic Slope Current (ASC), a strong, narrow current along the continental slope. The ASC exhibits as strong temperature gradient, and is also coined the Antarctic Slope Front (ASF), which acts as a barrier between the open ocean and shelf waters (Thompson et al., 2018; Huneke et al., 2022; G. Williams et al., 2010). Where DSW is exported over the continental shelf break, the isoneutrals in this front shoal, creating a "V" shape (Marsland et al., 2004). This is known as a dense shelf regime, and allows for the intrusion of the warm ($\sim$1°C) and salty CDW onto the continental shelf (Dinniman et al., 2016; Bindoff et al., 2000). The three AABW formation regions also observe an intrustion of CDW via a large, clockwise circulation around the embayments. Once on the shelf, CDW mixes with shelf water masses to become modified CDW (mCDW) (Cougnon et al., 2013). This mixing of water masses influencing the shelf water properties and local processes that lead to DSW formation and export in the region (e.g. driving increased Ice Shelf Water (ISW) formation) (Orsi & Wiederwohl, 2009; Foldvik et al., 2004; G. D. Williams et al., 2010).

As a result of variations in the processes above, each of the four regions produce DSW with slightly different characteristics. Cape Darnley creates the highest absolute salinity DSW reaching up to 35.07 g/kg, with the Ross Sea and Adélie Land DSW both exhibiting salinities of 34.9 g/kg (Silvano et al., 2020; G. D. Williams et al., 2010; Ohshima et al., 2013). The freshest DSW is exhibited in the Weddell Sea, with a salinity of 34.87 g/kg, due to the presence of cold and fresh ISW from the Filchner Depression and the western shelf (Foldvik et al., 2004; Darelius et al., 2023).

Once DSW has formed, and is of sufficient density, it flows down the continental slope via export pathways (down canyons or as cascading plumes, eddies, or gravity currents). G. D. Williams et al. (2010) found that calculating a quantitative critical density for DSW that leads to AABW is not plausible as it varies greatly by region, within regions, and interannually. Within each region, there is evidence for a split in DSW export exhibiting a high salinity and low salinity variant (Wang et al., 2012; G. D. Williams et al., 2010).

The exported DSW is altered by the entrainment of ambient offshore water masses, primarily CDW, creating a warmer, less dense, modified Shelf Water (mSW) on the slope. As mSW continues to descend, it entrains more CDW, eventually becoming AABW, defined as having a neutral density of 28.27 kg/m$^3$ or greater (Bindoff et al., 2000; Ohshima et al., 2013). On the sea floor, the thermobaric effect causes temperature to become the dominant component of the AABW neutral density (G. D. Williams et al., 2010). For each formation location the AABW temperature differs depending on the formation process. For example the upper temperature boundary for this density gradient is the lowest in the Weddell Sea region with a conservative temperature of -0.7°C, due to the role of ISW (Wang et al., 2012). The Ross Sea and Adélie Land have similar upper boundary temperatures of -0.1°C and 0°C respectively (Budillon et al., 2011; G. D. Williams et al., 2010).

### 2.1 Cape Darnley Bottom Water Formation

Cape Darnley is located in East Antarctica, west of the Prydz Bay and Amery Ice Shelf, ranging between 64 to 69.5°E. The cape and a grounded ice barrier (Cape Darnley Ice Barrier) block the westward movement of sea ice, creating ideal conditions for the Cape Darnley Polynya to form over the MacRoberston Land continental shelf. However, the region was initially dismissed as a potential region for AABW formation as this area does not have a large embayment and basin like the Ross, Weddell and Adélie regions, instead it has a shallow, narrow continental shelf ($\sim$90 km), with a large portion of the polynya lying directly over the shelf break and upper slope (Figure 1)(Ohshima et al., 2013, 2016).

The discovery of DSW export from the Cape Darnley Polynya highlighted that the criteria previously believed necessary for DSW and AABW formation may not apply to all regions. Despite the narrow shelf, the DSW formed here achieves the required density to form AABW, attributed to the high sea ice production in the polynya (Ohshima et al., 2013, 2016). The Cape Darnley Polynya has the smallest area (13000 $\pm$ 1600 km$^2$) of the four AABW polynya sites, however, it has the second highest sea ice production rate (182 $\pm$ 23 km$^3$/yr) (Tamura et al., 2016). A recent study by Ohshima et al. (2022) also suggests that frazil ice up to 80 m below sea level dominates in the polynya. This further facilitates efficient sea ice production and prevents thick sea ice from forming (Ohshima et al., 2022). The DSW in this region reaches a minimum salinity in May, and becomes the dominant water mass on the shelf between August and October (Portela et al., 2022). However, DSW seasonality in the Cape Darnley region is still difficult to assess due to limited sampling and data (Portela et al., 2022).

To the east of Cape Darnley, Prydz Bay was initially thought to be a good candidate for a forth region of AABW formation as it contains three active polynyas (Mackenzie, Davis, and Barrier). The DSW formed in Prydz Bay does not reach sufficient density for export due to mixing processes with ISW from the Amery Ice Shelf (G. D. Williams et al., 2016; Cougnon et al., 2013; Ohshima et al., 2013; Mizuta et al., 2021). However, the westward flow of cooler water masses play an important role in preconditioning the Cape Darnley region shelf waters. It is likely that Prydz Bay DSW flows westward along the slope after descending the Prydz Channel (Nunes Vaz & Lennon, 1996; G. D. Williams et al., 2016). However, recent studies by Portela et al. (2021) conflict with this, suggesting DSW formed in Prydz Bay flows east due to gravity driven flows. Despite the contested extent of DSW preconditioning, the adjacent Prydz Bay region plays an important role in prescribing the water mass properties on the Cape Darnley shelf.

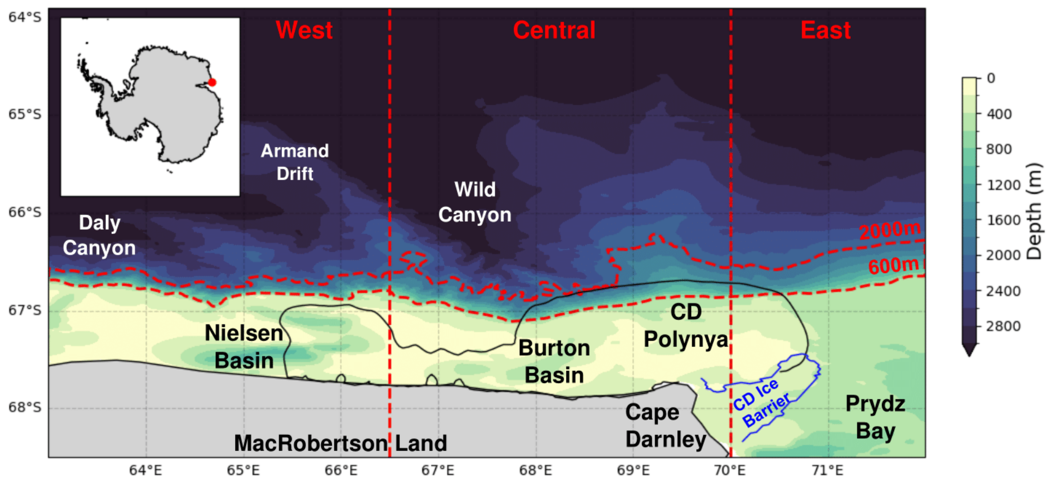


Figure 1: Cape Darnley study site with sea floor bathymetry.The black solid line shows the Cape Darnley polynya and the blue solid line shows the location of the Cape Darnley Ice Barrier (defined in section 3.0). The red dashed lines indicate the boundaries for the nine regions (defined in section 3.1) at the 600 m & 2000 m isobaths, 66.5°E and 70°E.

DSW formed in Cape Darnley is exported via the Wild and Daly Canyons. It descends to greater depths with the aid of thermobaricity and the steep continental slope to form CDBW (Ohshima et al., 2013). This steep slope at Cape Darnley is another key difference in the region, theorised to allow DSW to descend with less modification from ambient water masses, preventing the need for accumulation within a shelf basin (G. D. Williams et al., 2010). CDBW contributes 6-13% (2.13 Sv) of total AABW (Kusahara et al., 2010; Ohshima et al., 2013). Many studies have been conducted on CDBW since its discovery (Ohshima et al., 2013; Herraiz-Borreguero et al., 2015; Tamura et al., 2016; G. D. Williams et al., 2016; Fraser et al., 2019; Aoki et al., 2020; Gao et al., 2022; Guo et al., 2022; Ohashi et al., 2022; Ohshima et al., 2022; Portela et al., 2022; Bourreau et al., 2023). However, most of these studies focus on one aspect of the region, or use data with limited spatial or temporal resolution. In this paper we compile all the available hydrographic data from CTD, autonomous float and seal CTD over the last 40 years to provide the first ocean climatology of the Cape Darnley and western Prydz Bay region and new insights into the formation of DSW and AABW in this region. Understanding the current oceanic conditions at Cape Darnley is vital for monitoring and modelling experiments to assess the role climate change is having and will have on this system in the future.

## 3 Oceanographic data & Methodology

For this study, data within the Cape Darnley and western Prydz Bay region (defined as 65–68.5°S and 63–73°E) were collated over the past 40 years. This included data from ships, autonomous floats and instrumented southern elephant seals (*Mirounga leonina*; see Supp. Figure S1). All data sets were converted to TEOS-10 standards (i.e. absolute salinity, conservative temperature and neutral density) for comparison (IOC, SCOR and IAPSO, 2010). The resultant data product can be found at `10.5281/zenodo.10976304` (Blanckensee, 2024).

The different sources and methods of data collection have varying levels of instrument uncertainty (see Table 1). These datasets have all undergone post-processing before being released publicly (McMahon et al., 2023; Boyer et al., 2018; Ohashi et al., 2022). Nevertheless, further quality control was manually completed during the collation process. We removed data that exceeds reasonable bounds of temperature, salinity and oxygen (> 3 standard deviations from mean), which was primarily present in older ship datasets. Despite the inherent uncertainty in seal measurements, our analysis revealed a high degree of agreement between the seal dataset and the data obtained from ships and floats, as depicted in Supp. Figure S2. However, seal data does have an extra uncertainty in spatial location, with a median error of 3.2 km (McMahon et al., 2023). In order to take into account this spatial uncertainty, we chose to make our gridded analysis cells greater than this distance (0.1° by 0.1°).

An added layer of uncertainty in this combined ship, float and seal data set is the temporal variability resulting from collation of multi-year and -seasonal data into a single dataset. The variability introduced through combining multiple seasons into a single dataset can be observed in Figure 4 which displays data 0.5 standard deviations either side of the mean. The surface waters exhibit the greatest seasonality and hence greater variability, owing to their direct interaction with the atmosphere. However, a seasonal analysis of this region has previously been conducted by Portela et al. (2021) and the focus of this paper lies primarily on intermediate and bottom waters. Consequently, all seal data was included to increase the spatial coverage of the region. The collated dataset is also strongly biased to the last 15 years, as there was limited data collected prior to this time.

Table 1: Overview of data sources, ranges and measurement error (Ohashi et al., 2022; Boyer et al., 2018; Sea-Bird Scientific, 2023, 2024; National Institute of Polar Research, 2009; McMahon et al., 2023; MEOP, 2015)

| **Type** | **Years** | **Range** | | | **Data source** | **Measurement error** | | | |
|---|---|---|---|---|---|---|---|---|---|
| | | **Spatial** | **Temporal** | **Depth** | | **Salt (S·m-1)** | **Oxy (%)** | **Press** | **Temp (°C)** |
| Ships | 1981 – 2023 | Shelf (limited), slope & offshore | Primarily summer | Sea floor | WOD, AAD, CCHDO, RDA, NIPR | 0.0002 – 0.003 | 2 | 0.015 – 0.08% FS | 0.001 – 0.005 |
| Floats | 2009 – 2023 | Slope & offshore | All seasons | Core <2000m, Deep <4000m | WOD | 0.0005 – 0.001 | 2 – 5 | 2.4db | 0.002 |
| Seals | 2011 – 2019 | Shelf (primarily), slope & offshore | | <1600m | MEOP | 0.003 | - | 0.015% FS | 0.03 |

[1] median locational error seal data = 3.2 km

We sourced gridded bathymetry data from GEBCO v2023 (GEBCO Compilation Group, 2023). The fast ice and sea ice production contour outlining the Cape Darnley Polynya position was calculated from Tamura et al. (2016) product. The polynya contour delineates the 60 W/m$^2$ annual mean ocean heat loss (based on sea ice production contours used in Ohshima et al. (2013) and G. D. Williams et al. (2016)) and the fast ice boundary represents where ice is present for 95% of year (Tamura et al., 2016) product.

### 3.1 Analysis techniques

Water masses were first classified into three layers based on neutral density definitions previously identified by Orsi et al. (1999): surface, intermediate, bottom (<28.00, 28.00–28.27, >28.27 kg/m$^3$) (see isoneutrals in Figure 2). Depth, salinity and temperature conditions were then used to further classify the water masses based on previous studies of hydrographic characteristics from around East Antarctica (Herraiz-Borreguero et al., 2015, 2016; G. D. Williams et al., 2016; Orsi & Wiederwohl, 2009; Portela et al., 2021).

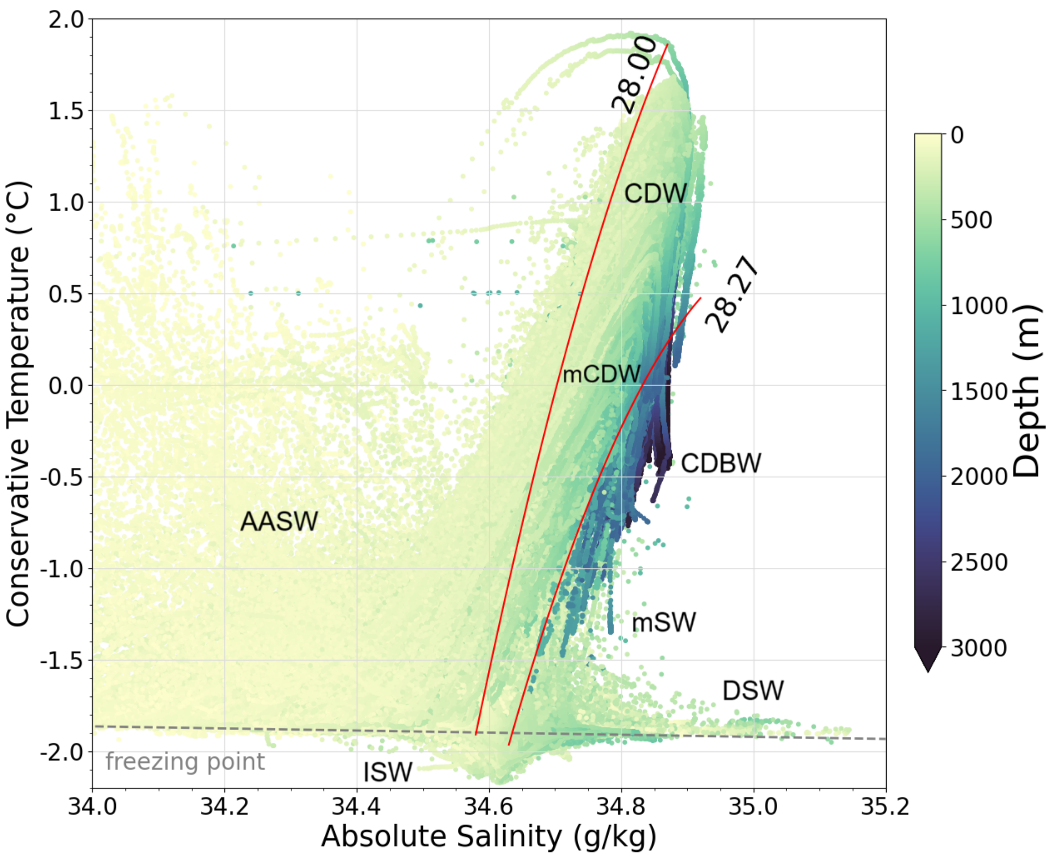


Figure 2: All data sources (ship, autonomous float & seal) in conservative temperature - absolute salinity space coloured by depth. The surface freezing point is represented by the gray dashed line and the 28.00 & 28.27 kg/m$^3$ neutral density lines are in red (see Supp Figure S2 for split in data between, ships, autonomous floats & seals).

The gridded spatial plots provide another insight into the region. For each individual cast, the mean absolute salinity and conservative temperature value was calculated for each density layer. The thickness of this layer was determined using the upper and lower depth values that fall within the density layer. The ship and float datasets have similar depth resolution (every 1–2 m). However, the depth resolution of seals varies with depth (i.e. 2.5 m for depths between 2.5–35 m; up to 25.0 m for depths between 420–1500 m). Although this may introduce slight discrepancies in the calculations due to its varied bin sizes, the dataset provides valuable insights into the shallower waters (<1000 m) on shelf and slope regions where there is limited CTD and float data. Then, to remove bias through over-plotting of co-located data, a 0.1° by 0.1° grid was created, with the mean of all points that fall within a cell displayed in Figures 5, 6 and 7 where each step represents 1/8th of the data points. Due to the data scarcity in this region, we have not excluded any grid cells based on a minimum data count to provide a more complete oceanographic representation of the region.

From this gridded analysis and bathymetry patterns, data was then partitioned into nine key regions for temperature-salinity and mean analysis. To capture shelf, slope and offshore processes, three zonal bands were identified: **shelf (<600 m depth)**, **slope (between 600–2000 m depth)** and **off-shore (north >2000 m depth)**. Then, to capture water mass changes along the coastline, three meridional bands were identified: **east – 70-72°** (western Prydz Bay / east of Cape Darnley), **central – 66.5-70°E** (highest sea ice production in the Cape Darnley Polynya and over the Burton Basin), and **west – 63-66.5°E** (lowest sea ice production in the Cape Darnley Polynya and over the Nielsen Basin).

To develop latitudinal depth transects, we identified the most recent offshore shipboard CTD transects within each meridional sector at 65°E, 68°E, and 70°E. These were then extended on to slope and shelf using any data source (ship, float, or seal) that fell along these longitudinal lines (excluding winter to minimise seasonal variation). Data were then linearly interpolated between points for spatial coherence.

# 4 Results

The following results have been partitioned into shelf, slope and offshore processes as each latitudinal band has distinct characteristics. These are then split into the surface, intermediate and bottom water masses, which are also discussed by the meridional sector location (east, central, and west).

## 4.1 SHELF (bathymetry <600 m)

### *4.1.1 Surface water masses ($y^n$ < 28.00 kg/m$^3$)*

On the continental shelf, AASWs have high variability (Figure 3g–3i) with temperatures ranging from -1.95°C to ∼1.0°C, and salinities ranging from 32 to 34.7 g/kg. East of Cape Darnley in the upper ∼200 m, AASW temperatures are the coldest (sitting along the surface freezing point of -1.95°C) and saltiest (∼0.4 g/kg higher than the sectors east of Cape Darnley) (Figure 4g & 4h). In the eastern sector, oxygen content also peaks (320 < O < 360 $\mu$mol/L) (Figure 4i). This cold (-1.95 < $\theta$ < -1.38 °C) and salty (34.3 < S_A < 34.72 g/kg) AASW is also evident in Figure 5a & 5b. Here, AASW has a thickness of 0 to ∼191 m, with the thinnest AASW east of the 71°E (Figure 5c). There is an isolated patch of thick AASW between 70–70.8°E and south of 68°S, with a thick (85 < T < 191 m), narrow, layer flowing along the 400 m isobath along the Prydz Channel to the edge of the slope.

Moving to the west the coldest (-1.95 < $\theta$ < -1.58 °C) and saltiest (34.42 < S_A < 34.72 g/kg) waters within the Cape Darnley Polynya are present in its north-east portion, similar to that in Prydz Bay (Figure 5). However, there is a sharp gradient in temperature and salinity along a line from (67.5°S, 68°E) to (67.8°S, 69.2°E). South-west of this line waters in the Cape Darnley Polynya are fresher (32.04 < S_A < 34.37 g/kg) and warmer (>-1.58°C). Overall, the central sector AASW exhibits the lowest oxygen content (260 < O < 330 $\mu$mol/L) (Figure 4i). Transitioning into the western sector, sea ice production in the Cape Darnley Polynya is lower than the central sector (Ohshima et al., 2013) and AASW gradually thickens (0 < T < 685 m), becomes fresher (33.95 < S_A < 34.65 g/kg), and warmer (-1.7 < $\theta$ < -1.3 °C) (Figure 4g – h & 5). There are also two thick (150 < T < 290 m), narrow, branches of AASW overlying the Nielsen and Burton Basins (Figure 5).

### *4.1.2 Intermediate water masses (28.00 < $y^n$ < 28.27 kg/m$^3$)*

On the shelf, water that falls into the intermediate density class is either mCDW, or falls along the mixing line between AASW and DSW. A lower temperature bound for mCDW has previously been defined as 0.1°C above the surface freezing point, but water along the mixing line can also exceed this temperature threshold (Portela et al., 2021). In this study, to differentiate mCDW and water along the mixing line, we use a lower temperature bound of approximately -1.2°C for mCDW. This temperature bound was determined from a discernible curve in the temperature-salinity plot that marks the transition from AASW to DSW, with an inflection point at approximately -1.2°C (Figure 3g–3i). Water parcels warmer than this threshold exhibit characteristic mCDW properties (warmer and saltier with mid range depths).

In the eastern sector, this intermediate layer is the thickest of the meridional regions (18 < T < 197 m) (Figure 6c). These intermediate waters exhibit lower temperatures (-1.95 < $\theta$ <-1.59°C) and sit along the mixing line with the thickest waters found directly east of the Cape Darnley Ice Barrier. A small amount of mCDW is found just south of the 600 m isobath line at approximately 67.1°S, with temperatures between -1.59 and -0.27°C (Figure 6).

West of 69°E, this intermediate layer sits below a depth of ∼150 m and thins rapidly polewards towards the coastline (from 591 m to <18m). mCDW intrudes onto the shelf via the Nielsen and Burton Basins where there is a relatively thick (18 < T < 98 m) layer of warmer (-1.59 < $\theta$ < -0.27 °C) and saltier (34.64 < S_A < 34.74 g/kg) water which intrudes as far south as 67.4°S (Figure 6).

#### *4.1.3 Bottom water masses ($y^n$ > 28.27 kg/m$^3$)*

The bottom density layer principally captures DSW, which is present as a thin (<122 m) layer across the entire shelf (Figure 7). It exhibits temperatures near the surface freezing point (-1.95 < $\theta$ < -1.85 °C) and salinities >34.65 g/kg (Figure 3g–3i). The thickest (> 122 m) and largest volumes of DSW are found in the Nielsen Basin, Burton Basin, directly north of Cape Darnley and in Prydz Bay to the east (Figure 7c).

In the eastern sector, Prydz Bay DSW is the coldest (-2.16 < $\theta$ < -0.72 °C), freshest (34.62 < S_A < 34.81 g/kg) (Figure 3g & 3h) and most oxygenated (∼320 $\mu$mol/L) (Figure 4i). However, ISW is also present within this density layer in the eastern sector as indicated by temperatures below the surface freezing point (-2.15 < $\theta$ < -1.95°C) and low salinities ( 32.51 < S_A < 34.62 g/kg) in front of the Amery Ice Shelf (Figure 3g–3i & Supp. Figure S3).

In the central shelf sector, DSW is the warmest (-1.6 < $\theta$ < -1.0 °C) and saltiest (up to 34.9 g/kg) (Figure 4g–4h & 7). This sector also records the highest singular salinity measurement, reaching 35.15 g/kg (Figure 3h). This salty DSW is found along the coastline and follows the Burton Basin towards the shelf break. Oxygen in this sector is the lowest of the three shelf sectors, reaching a minimum of 215 $\mu$mol/L (Figure 4i).

The western sector DSW is, on average, slightly cooler (-1.95 < $\theta$ < -1.5 °C), and fresher (up to 34.85 g/kg) in comparison to the central sector. This DSW can be observed around 65°E at the base of the Nielsen Basin at depths between approximately 400–1000 m (Figure 4g & 4h). Oxygen content in this sector falls between the east and central sectors (290 < O < 300 $\mu$mol/L (Figure 4i).

### 4.2 SLOPE (bathymetry 600–2000 m)

#### *4.2.1 Surface water masses ($y^n$ < 28.00 kg/m$^3$)*

AASW over the slope exhibits very similar thermohaline characteristics to those of the shelf region in the top 150 m across the three meridional sectors, albeit with a slightly higher temperature (+0.2°C) for the top 50 m (Figure 4d and 4e). The AASW is also slightly less oxygenated than on the shelf region (∼330 < O < ∼350 $\mu$mol/L from east to west) (Figure 4f).

The ASC is recognisable along the shelf break, by a thick (> 197 m) layer of AASW with mid-range temperatures (-1.77 < $\theta$ < -1.38 °C) and variable salinities (Figure 5). It is most prominently observed between 68°E to 70.5°E where the ASC is wider, covering a broader latitudinal range.

#### *4.2.2 Intermediate water masses (28.00 < $y^n$ < 28.27 kg/m$^3$)*

The ASC is also evident in the middle density layer. A thick (197 < T < 591 m) layer of CDW is found along the entire slope with mid-range temperatures (-0.27 < $\theta$ < 0.43 °C) and mid-range salinity (34.74 < S_A < 34.85 g/kg) (Figure 6). This layer is also widest between 68°E to 70.5°E (Figure 6 & Figure 8).

As with the shelf profiles, salinity increases, and oxygen content decreases with depth (Figure 4d–4f). However, while the shelf temperature is mostly uniform from the surface to the sea floor, the mean temperatures on the slope slowly increase with depth from a minimum at 50 m, peaking at ∼600 m.

In the eastern sector at this inflection depth (∼600 m), CDW is warmer (∼0.6°C) and saltier (∼34.85 g/kg). This sector also observes the lowest CDW oxygen content of ∼185 μmol/L (Figure 4d–4f). Prydz Bay also exhibits a fresh shelf regime as the 28.00 kg/m$^3$ isoneutral has a high angle of intersection with the continental slope (from ∼125 m to ∼300 m) and a flatter density surface than the western sectors (Figure 8e & 8f).

The central sector observes very similar temperature and salinity peaks to the eastern sector, only ∼0.1 °C and ∼0.05 g/kg below the eastern sector (Figure 4d–4f). Here, the 28.00 kg/m$^3$ isoneutral has a lower angle of intersection with the continental slope, tilting from ∼175 m to ∼275 m (Figure 8c & 8d). However, there is a slight shoaling exhibited near the continental slope, creating a slight "V" feature.

In the western sector, the 28.00 kg/m$^3$ isoneutral displays the "V" feature of the ASF, indicative of a dense shelf region (Figure 8a & 8b) (Gill, 1973; Jacobs, 1991; Thompson et al., 2018; Whitworth et al., 1985). There is also a steep drop in mean temperature, paired with an increase in mean oxygen at the inflection depth, but no noticeable change in salinity (Figure 4d–4f). Hence, this sector observes the lowest minimum temperature (∼-0.7°C) and salinity (34.8 g/kg) with the highest oxygen content (275 μmol/L).

#### *4.2.3 Bottom water masses ($y^n > 28.27$ kg/m$^3$)*

The bottom density layer on the slope represents mSW. All sectors observe a gradual decrease in temperature and increase in oxygen from 600 to 2000 m depth, while salinity remains fairly constant (Figure 4d–4f). Exported DSW from the shelf region entrains warmer, saltier, offshore water masses, forming warmer (-1.82 < $\theta$ < -0.09 °C) and saltier (34.70 < S_A < 34.84 g/kg) mSW (Figure 7). This mSW signal is also carried westward along the slope from ∼68°E. mSW has a neutral density greater than 28.27 kg/m$^3$, temperature >-1.8°C and <∼-0.7°C, at depths of ∼500 m to 2000 m.

### 4.3 OFFSHORE (bathymetry >2000 m)

#### *4.3.1 Surface water masses ($y^n < 28.00$ kg/m$^3$)*

Offshore, surface climatology is more homogeneous across the three meridional sectors compared to surface conditions on the shelf and slope (Figure 4a–4c). The greatest variation is exhibited in the eastern sector where the top 150 m has ∼20 μmol/L lower oxygen content compared to the central and western sectors. In contrast, the western sector has slightly warmer (+ ∼0.3°C) and fresher (- ∼0.05 g/kg) conditions.

#### *4.3.2 Intermediate water masses ($28.00 < y^n < 28.27$ kg/m$^3$)*

Below 150 m offshore, temperatures and salinity slowly rise, peaking at ∼500 m. This mid-depth peak is warms (0.6 < $\theta$ < 0.8 °C) from east to west, with similar, but more homogenous salinity (34.84 < S_A < 34.87 g/kg) across the three meridional sectors than found on the slope. Oxygen is also more uniform at these mid-range depths compared to the slope region (∼200 < O < ∼210 μmol/L from east to west) (Figure 4a–4c).

Offshore of Cape Darnley CDW is found spanning the entire study site offshore (150 < depth < 1500 m) as warm (0.2 < $\theta$ < 1.46 °C) and salty (34.71 < S_A < 34.89 g/kg) water (Figure 6). Lower CDW is bounded by the 28.00 and 28.27 kg/m$^3$ isoneutrals, with upper CDW bounded by 27.80 and 28.00 kg/m$^3$ isoneutrals. The upper CDW tongue is observed further south in the western transect, reaching ∼65°S, in comparison to ∼64°S in the central and eastern sectors (Figure 8). This aligns with the warmer mid depth conditions found to the west (Figure 4a).

#### *4.3.3 Bottom water masses ($y^n$ > 28.27 kg/m$^3$)*

Offshore, the bottom density layer is primarily AABW and is found below 1000 m with a neutral density >28.27 kg/m$^3$ (Figure 3a–3c). It can also be identified by a sharp increase in oxygen content at depth, observed in all three sectors (Figure 4a–4c).

Data from this bottom density layer are sparse and do not always reach the seafloor. Therefore, mean thickness calculations are underestimated and unreliable offshore. However, by using bottom of cast data, the temperature (-1.27 < $\theta$ < 1.47°C) and salinity (34.70 < S_A < 35.15 g/kg) range can be identified (see Supp. Figure S4).

There are three shipboard CTD transects that show the upper bound of temperature along the 28.27 kg/m$^3$ isoneutral is ∼0.05°C and salinity upper bound is ∼34.845 g/kg (Figure 8). The transects also show that between the eastern and western transects (both taken in 2021), there is little difference in the thickness of AABW (both ∼1000 m thick). In comparison, AABW in the central transect (taken in 1992) is thicker (∼1400 m thick) than the 2021 transects.

There is also variation in the position of the 28.27 kg/m$^3$ isoneutral on the continental slope. In the western and central transect, it is furthest up the continental slope, reaching a depth of ∼1000 m (Figure 8a – 8d), compared to the eastern sector where this isoneutral intersects with the slope bathymetry at a depth of ∼1700 m (Figure 8e & 8f).

Although AABW is found across all three offshore meridional sectors, its properties differ. Peak oxygen content (∼340 $\mu$mol/L) is found in the western sector, followed by ∼260 $\mu$mol/L in the eastern sector and ∼245 $\mu$mol/L in the central sector (Figure 4c). For both temperature and salinity, a minimum is found in the eastern sector (∼-0.75°C and ∼34.78 g/kg respectively) and a maximum is exhibited in the central sector (∼-0.3°C and ∼34.88 g/kg respectively) with the properties in the western sector falling between these values.

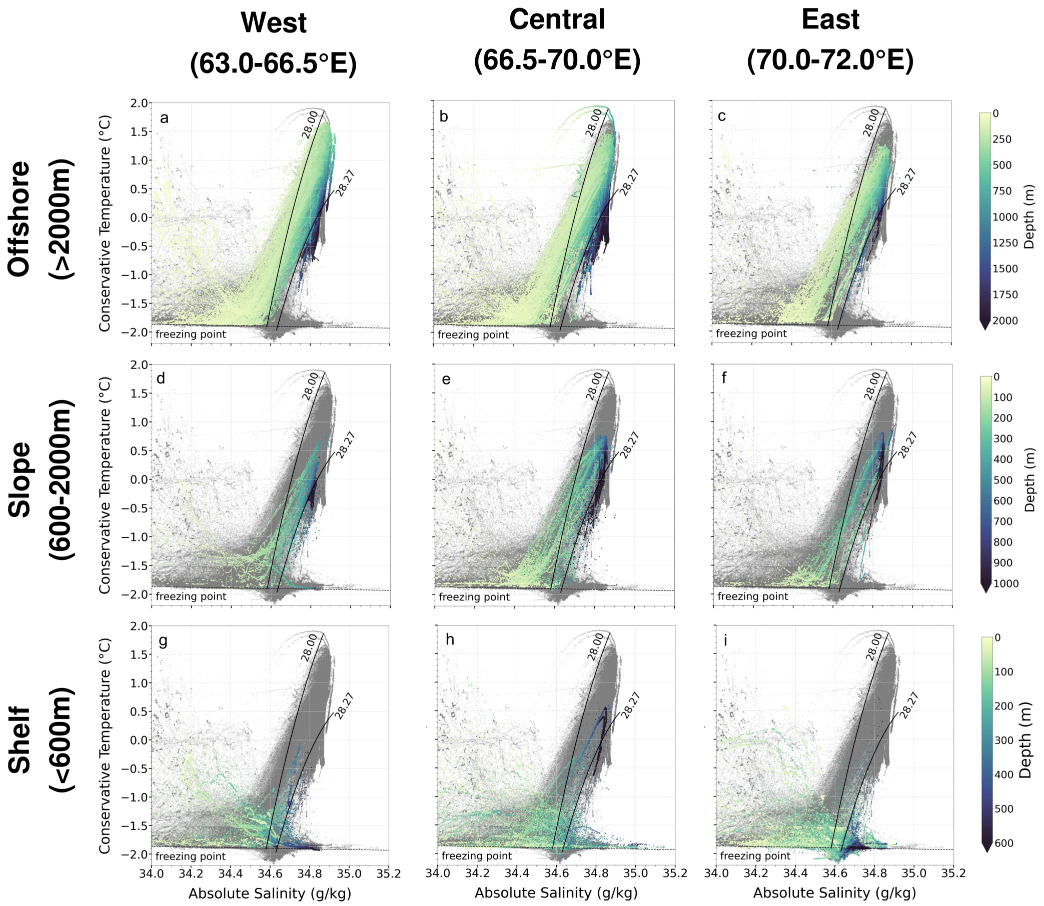


Figure 3: Conservative temperature vs absolute salinity plots for each of the nine sectors in this study, split into east (70-72°E), central (66.5-70°E) & west (63-66.5°E), and shelf (<600 m), slope (600–2000 m) & offshore (>2000 m). The two black lines indicate the 28.00 & 28.27kg/m$^3$ neutral density lines, with points in grey if they fall outside the sector, and coloured by depth if they fall within the sector. The surface freezing point is represented by the black dashed line

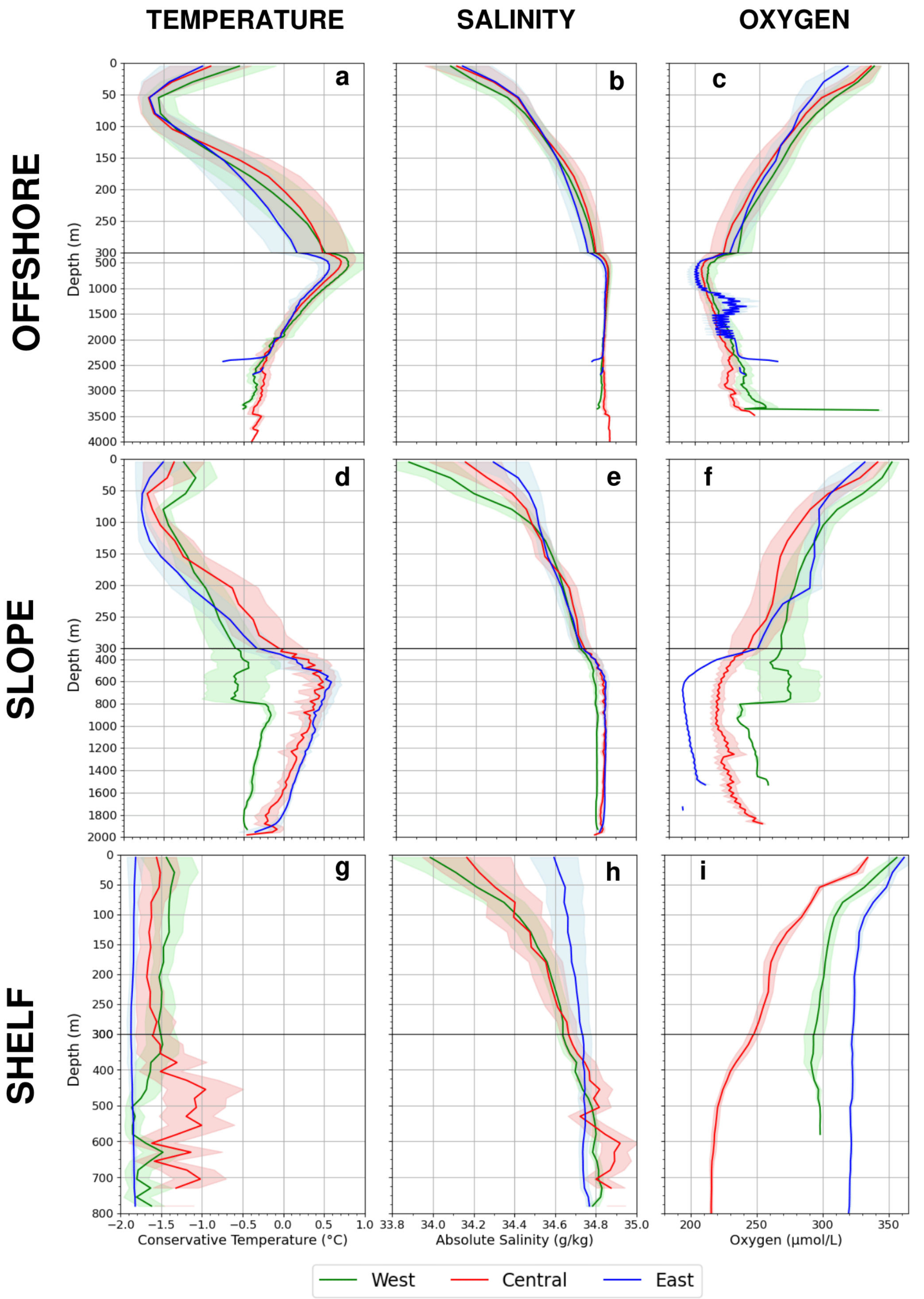


Figure 4: Depth profiles for offshore (a-c), slope (d-f) & shelf (g-i) split into west (green), central (red) and eastern (blue) regions for conservative temperature (a, d g), absolute salinity (b, e, h) and oxygen (c, f, i). The solid lines represent mean value of all data points in that sector every 25 m, with the lighter shaded colours surrounding the solid mean lines representing ±0.5 standard deviations to highlight seasonal & temporal variations.

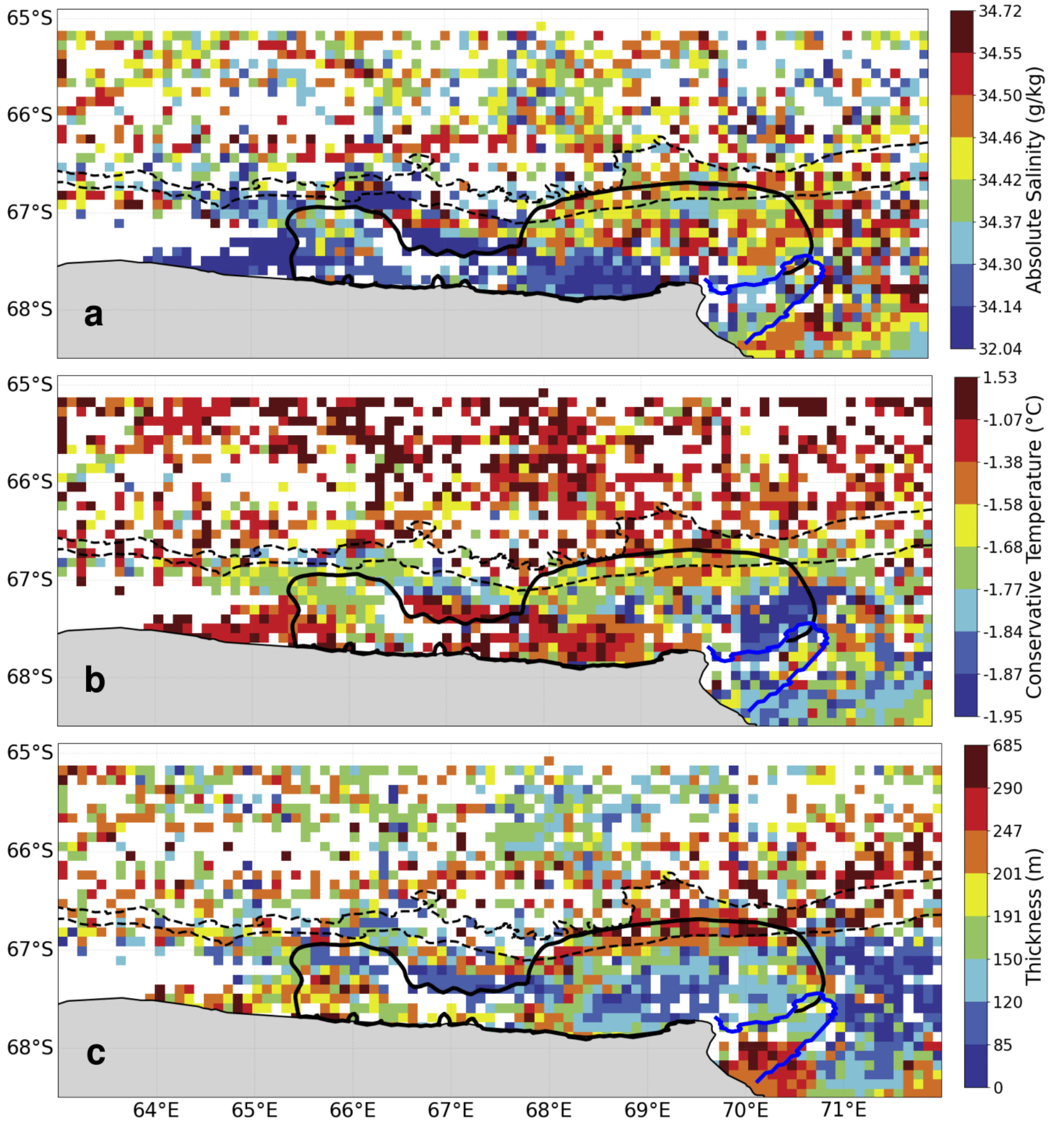


Figure 5: Gridded data of lightest density layer ($y^n < 28.00$ kg/m$^3$) for a) absolute salinity, b) conservative temperature & c) thickness. The black dotted lines represent the 600 m and 2000 m isobaths, the solid black line represents the polynya outline and the solid blue line represents the ice barrier.

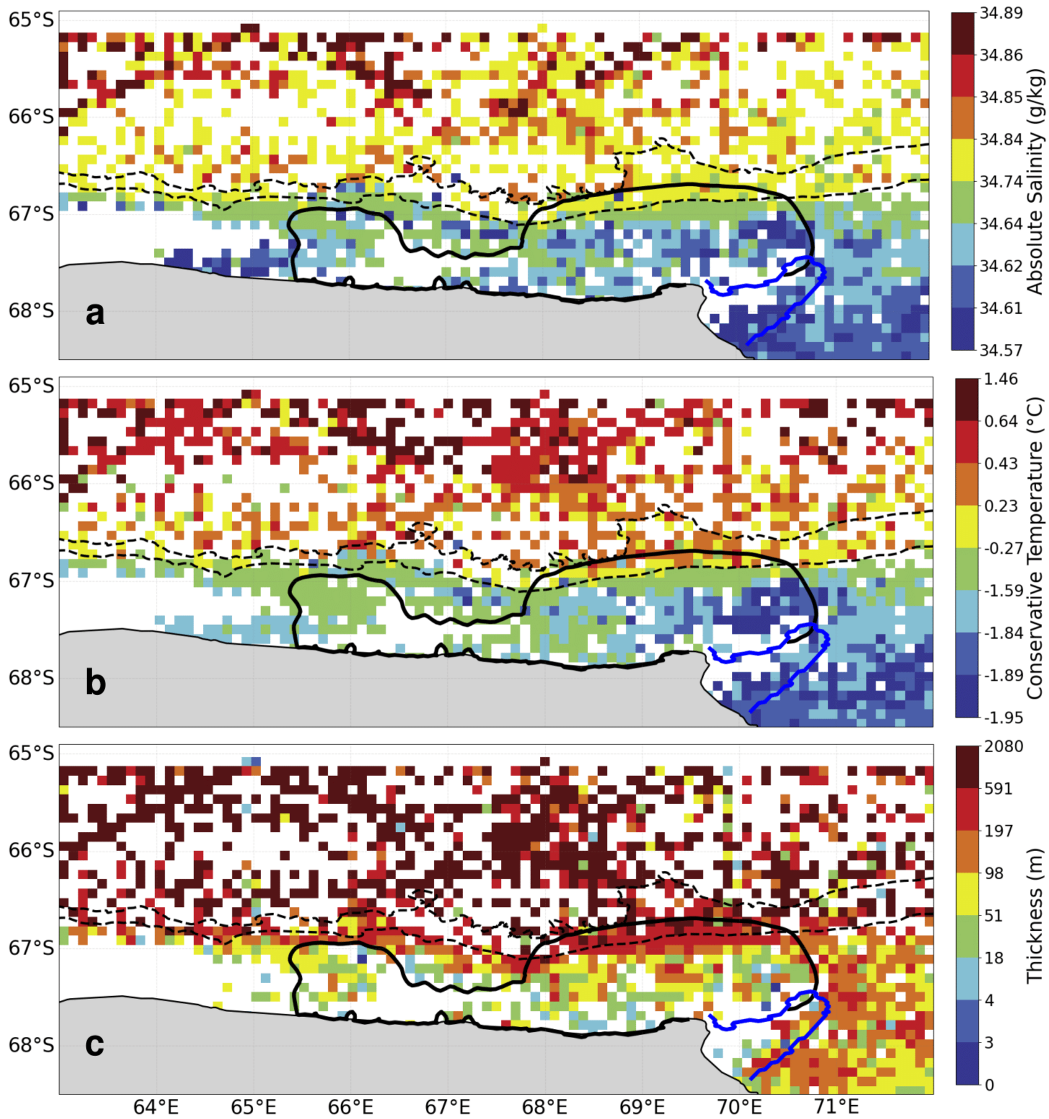


Figure 6: Gridded data of middle density layer ($28.00 < \gamma^n < 28.27$ kg/m$^3$) for a) absolute salinity, b) conservative temperature & c) thickness. The black dotted lines represent the 600 m and 2000 m isobaths, the solid black line represents the polynya outline and the solid blue line represents the ice barrier.

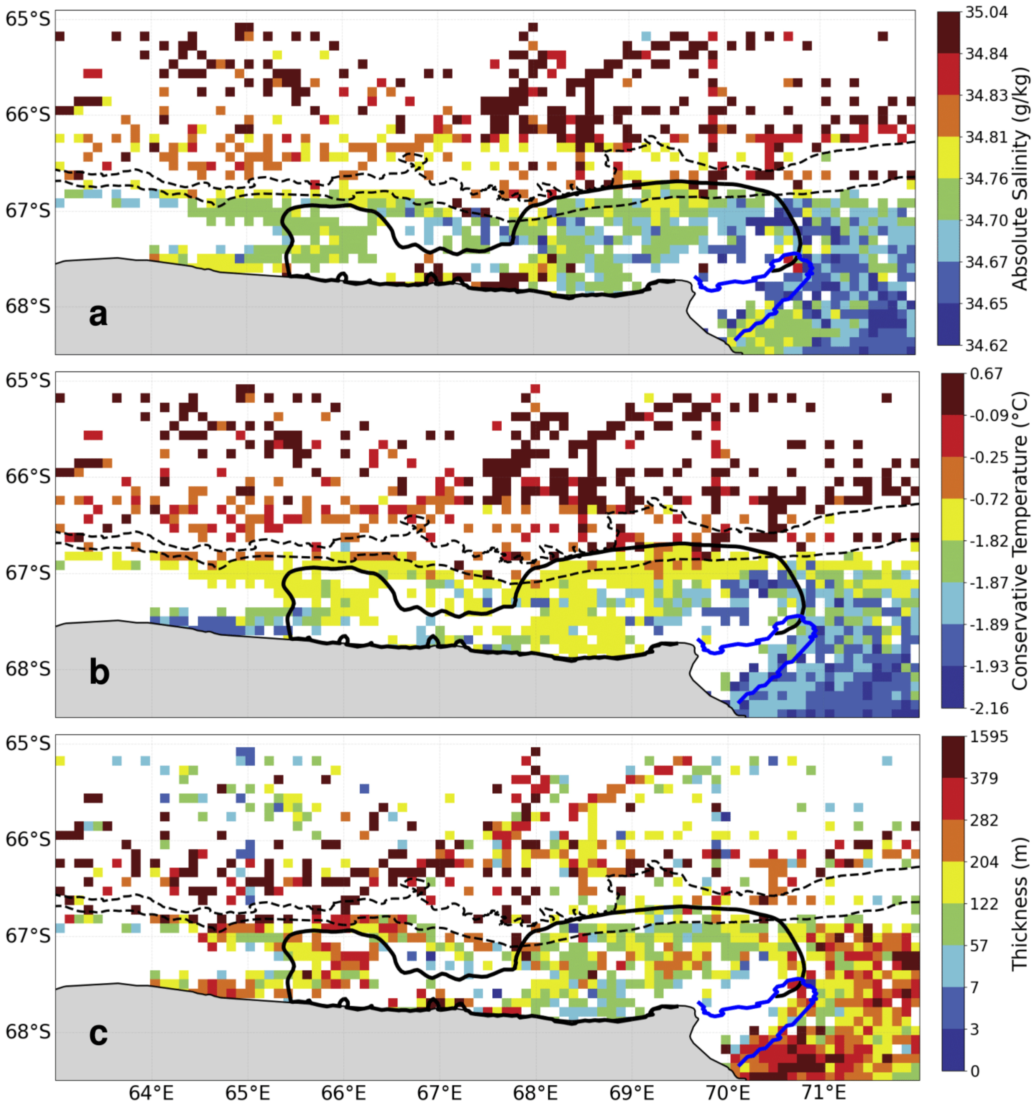


Figure 7: Gridded data of heaviest density layer ($y^n > 28.27$ kg/m$^3$) for a) absolute salinity, b) conservative temperature & c) thickness. The black dotted lines represent the 600 m and 2000 m isobaths, the solid black line represents the polynya outline and the solid blue line represents the ice barrier.

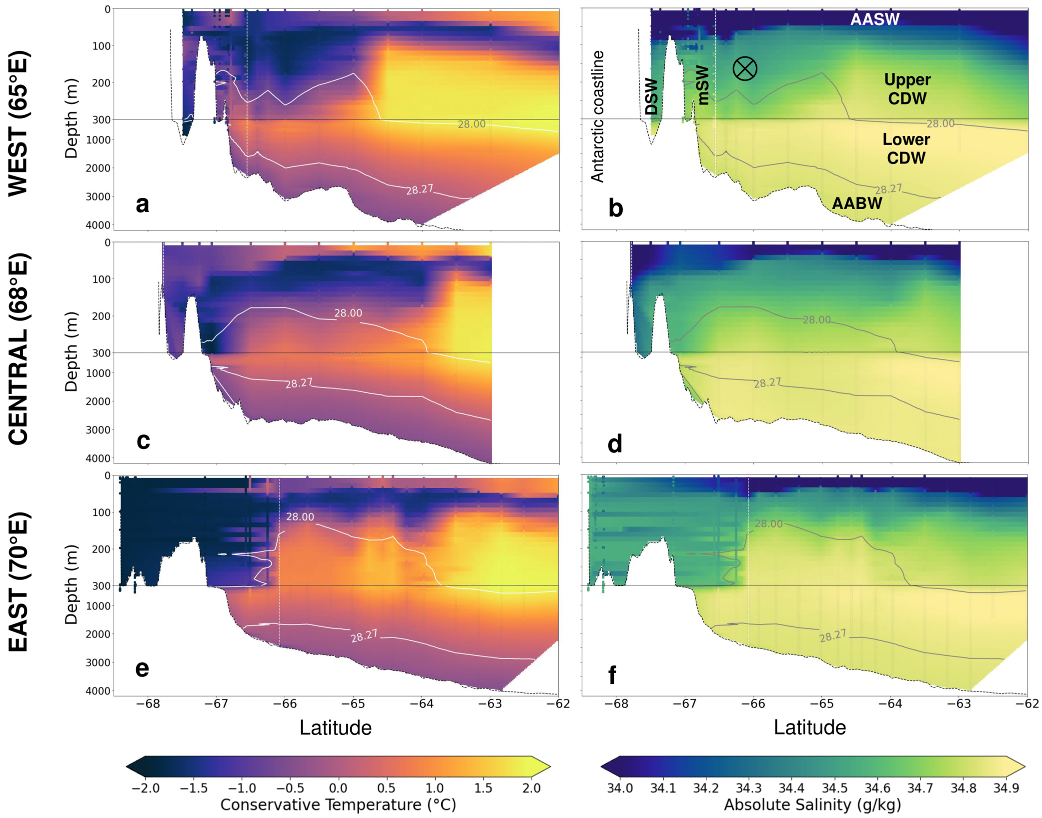


Figure 8: Meridional transects along the west (a & b), central (c & d), & and east (e & f) regions for conservative temperature(a, c & e) and absolute salinity (b, d & f). White/grey solid lines indicate the 28.00 and 28.27 kg/m$^3$ isoneutrals and the black cross circle indicates the approximate location of the Antarctic Slope Current. Interpolated data south of the vertical, dashed white line indicates where the continuous shipboard data for each transect ended and data was pooled from the entire dataset to complete the on shelf transect line. DSW = Dense Shelf Water, mSW = modified Shelf Water, AABW = Antarctic Bottom Water, AASW = Antarctic Surface Water, CDW = Circumpolar Deep Water

# 5 Discussion

## 5.1 Updated water mass classifications

Using this new compilation of oceanographic datasets for the Cape Darnley region, we propose an updated water mass classification for this region (see Table 2). The absolute salinity bounds were determined using the neutral density contours on the TS plot (Figure 3). Furthermore, we assign a lower temperature bound for mCDW of -1.2°C, to separate it from surface waters that fall within the intermediate density class which are following the mixing pathway to DSW (see Section 4.1.2).

Table 2: Updated mass classification for Cape Darnley, East Antarctica (updates highlighted in **bold**), adapted from Orsi et al. (1999); Orsi & Wiederwohl (2009); Portela et al. (2021). Updated temperature and salinity bounds were determined from Figures 2 & 8

| Neutral Density $y^n$ (kg/m$^3$) | Water Mass | Depth Range / Location | Absolute Salinity (g/kg) | Conservative Temperature (°C) |
|---|---|---|---|---|
| $y^n$ <28.00 | AASW | **<2000 m** | **<34.85** | >-1.95 |
| 28.00 <$y^n$ <28.27 | CDW | | **34.85 <S_A <34.90** | |
| | mCDW | | | **>-1.2** |
| - | ISW | **On shelf** | | <-1.95 |
| $y^n$ >28.27 | DSW | | **>34.62** | -1.95 <$\theta$ <-1.85 |
| | mSW | **Slope (600–2000 m)** | | >-1.85 |
| | AABW | **>1000 m** | **34.82 <S_A <34.85** | **<0.05** |

[1] Note: AASW = Antarctic Surface Water; CDW = Circumpolar Deep Water; mCDW = modified CDW; ISW = Ice Shelf Water; DSW = Dense Shelf Water; mSW = modified Shelf Water; AABW: Antarctic Bottom Water

## 5.2 Oceanic processes in the different meridional sectors of the Cape Darnley region

### *5.2.1 Eastern sector*

In the eastern sector, Prydz Bay Gyre observes unique shelf conditions. Here we observe the thinnest, coldest, and saltiest AASW. These attributes arise from the proximity of the Amery Ice Shelf, contributing cold water, and the mixing of saline mCDW that intrudes onto the shelf via the Prydz Bay cyclonic gyre (Portela et al., 2021; G. Williams et al., 2010) where we observe mCDW gradually increases in thickness to the east. The DSW formed from the Prydz Bay polynyas in this region is the coldest ($-2.16 < \theta <$ $-1.82$ °C) and freshest ($34.62 <$ S_A $< 34.76$ g/kg) of the meridional sectors due to the mixing with ISW formed under the Amery Ice Shelf (G. D. Williams et al., 2016). The resultant reduction in density means the DSW in this region does not reach the critical density to sink to the seafloor and become AABW and is the key reason Prydz Bay DSW is not the primary contributor to CDBW (Nunes Vaz & Lennon, 1996; G. D. Williams et al., 2016).

On the slope, a fresh shelf regime is observed. Here AASW is the thickest of the meridional sectors with a deepening of the 28.00 kg/m$^3$ isoneutral (Figure 8e & 8f). The high angle of intersection of this isoneutral with the continental slope indicates the presence of the ASC and the strongest frontal structure, classified as a fresh shelf regime by Thompson et al. (2018) and highlights that there is no/minimal active AABW formation (Meijers et al., 2010). Although the Prydz Bay region does not contribute DSW directly to CDBW formation, the cool, fresh DSW signal is found travelling wetward along the slope with the ASC, and the cool, salty AASW signal from Prydz Bay is found wrapping around the Cape Darnley Ice Barrier, preconditioning the waters in the Cape Darnley Polynya (Figure 9c & 9d) (Nunes Vaz & Lennon, 1996; G. D. Williams et al., 2016; Ohshima et al., 2013).

#### *5.2.2 Central sector*

The central sector is dominated by the Cape Darnley Polynya. At the surface, within the polynya, we found a sharp gradient in water properties across a line from (67.5°S, 68°E) to (67.8°S, 69.2°E), where north-east of this line has colder and saltier properties (Figure 5), indicating that the westward flow of AASW from Prydz Bay has a limited extent. These surface conditions may also indicate that the north-east portion of the polynya is more active, with greater exposure to the atmosphere, reducing surface temperatures and increased brine rejection. This observation is slightly different to sea ice production contours from 2008 published by Ohshima et al. (2013), that indicate the south-east portion of the polynya is the most active. However, our findings could also be supported as sea ice production in this north-east portion could also be aided by the Cape Darnley Ice Barrier (see blue outline in Figure 5), blocking the westward movement of ice, thereby maintaining the polynyas extent.

The combination of the preconditioned AASW and high sea ice production in the north-east portion of the polynya creates DSW that reaches the density required to form CDBW and does not need accumulation time in a shelf basin to achieve critical density (as seen in regions like the Adélie, Ross and Weddell Seas) (G. D. Williams et al., 2010). Some of this DSW likely directly flows onto the slope and downstream before descending Wild Canyon (Ohshima et al., 2013). However, the DSW from this active north-east portion and the less active south-west portion of the polynya in this sector also flows westward into Burton Basin (Figure 9b & 9d). Here we observe the highest salinity (up to 35.15 g/kg) DSW signal (Figures 3h & 7a), that we have coined Burton Basin DSW (Figure 9b & 9d). It must be noted that this dense water (below the 28.27 kg/m$^3$) is not observed in the interpolated transects on the central shelf (Figure 8c & 8d). This is likely a limitation of the method used to produce the shelf transect that introduced interannual/seasonal variability and greater horizontal interpolation, or alternatively the 68°E transect line may not lie along the lowest point of the basin, missing the DSW. Instead, we conclude that salinity peaks in this sector due to its proximity to the largest, most active portion of the polynya paired with preconditioning from Prydz Bay DSW.

The flow of Burton Basin DSW over the continental shelf changes the slope regime. This is highlighted by the shoaling of isoneutrals along the slope, creating a slight ”V” shape (Figure 8b). This shoaling also allows for warmer offshore CDW to intrude onto the shelf (as indicated in Figure 6b as water between -1.59 and -0.27°C) also via the Burton Basin. This sector was broadly categorised as a dense shelf regime by Thompson et al. (2018). However, the shape of the isoneutrals sit between those categorised for a fresh and dense shelf regime, therefore we redefine the central sector as a transitional regime. The ASC is visible along the upper slope as a thick layer of warmer AASW (Figure 5). North of Cape Darnley (between 68.8–69.5°E), there is an increase in the width of this current that may be the result of this region being more highly resolved by the dataset, alternatively it may also suggest that the more gradual incline of the slope bathymetry is causing the westward ASC to decelerate and form eddies due to the change in slope gradient. Hence, the ASF here is wider, represented by a more gradual incline of isoneutrals moving offshore compared to the eastern sector (Figure 8c & 8d).

Once the Burton Basin DSW has overflown the continental shelf, it descends down Wild Canyon (Ohshima et al., 2013). On the slope, it transitions into mSW as it mixes with offshore water masses before becoming CDBW at depths of ∼1000 m or greater (Figure 8c & 8d). We found AABW in the central sector is the shallowest and thickest observed across the three sectors. This could be a regional difference caused by variations in DSW production along the Cape Darnley shelf. However, it could also be a temporal difference as this central transect was collected in 1992, while the eastern and western transects were collected in 2021. Thus, the difference in thickness may be related to the freshening and contracting of AABW over 30 years (G. D. Williams et al., 2010; Tamura et al., 2008; Fogwill et al., 2015; Gunn et al., 2023). To better resolve the DSW and AABW spatial formation in the Cape Darnley region, contemporaneous transects across the three sectors would be required to remove temporal and seasonal variations for comparison.

#### 5.2.3 Western sector

The western sector shelf has similar oceanographic processes to the central sector. Here we found AASW on the shelf is the freshest and warmest, similar to the south-west portion of the polynya within the central sector, as the cold surface water from Prydz Bay appears to have little influence on this shelf sector. Instead, most of the westward flow of water from the eastern sector is found over the shelf break and slope in this western sector (Figure 5). Shelf AASW is thickest over the Nielsen Basin, reaching up to 640 m in this sector. This thick AASW close to the MacRobertson Land ice sheet could explain the small ISW signal observed along the coast (Supp. Figure S3). Beneath the polynya, DSW in this sector is primarily observed within the Nielsen Basin (Figure 7) which we have coined Nielsen Basin DSW. The DSW here is likely a combination of Burton Basin DSW that has flowed westward from the central sector and new DSW formed by the western portion of the polynya. This Nielsen Basin DSW has slightly fresher properties (maximum salinity of 34.85 g/kg) than that in the central sector (Figure 3g), with a different export pathway down the Daly Canyon (Figure 9a & 9d).

From the export of this DSW down the Daly Canyon, we observe a dense slope regime. An increase in slope oxygen and shoaling of the 28.00 kg/m$^3$ isoneutral indicate the presence of mSW on the slope, forming a distinct "V" configuration, indicative of a dense slope regime (Gill, 1973; Jacobs, 1991; Whitworth et al., 1985; Thompson et al., 2018). This "V" formation creates the steepest temperature gradient between the ASC and the offshore CDW tongue that protrudes the furthest south (to 64.5°S) in this sector, which aligns with the southernmost protrusion of the Antarctic Circumpolar Current (Meijers et al., 2010). The shoaling of isoneutrals along the slope also allows for CDW intrusion, which is exhibited as a thicker and warmer layer moving south, up the Nielsen Basin in this western sector (Figure 6b). The onshore mCDW intrusion is increased here due to the reduced sea surface height associated with DSW offshore pulses Morrison et al. (2020).

Offshore, the mSW is transformed into CDBW at depths >1000 m. Although the temperature and salinity properties of CDBW in this western sector sit between the central and eastern sector, oxygen content is ∼70 $\mu$mol/L above the other sectors. This is likely the result of DSW transport from the active central sector combined with DSW formation in the western sector. Thus, we suggest a higher volume of new CDBW is exported via the Nielsen Basin in the western sector compared to the Burton Basin in the central sector.

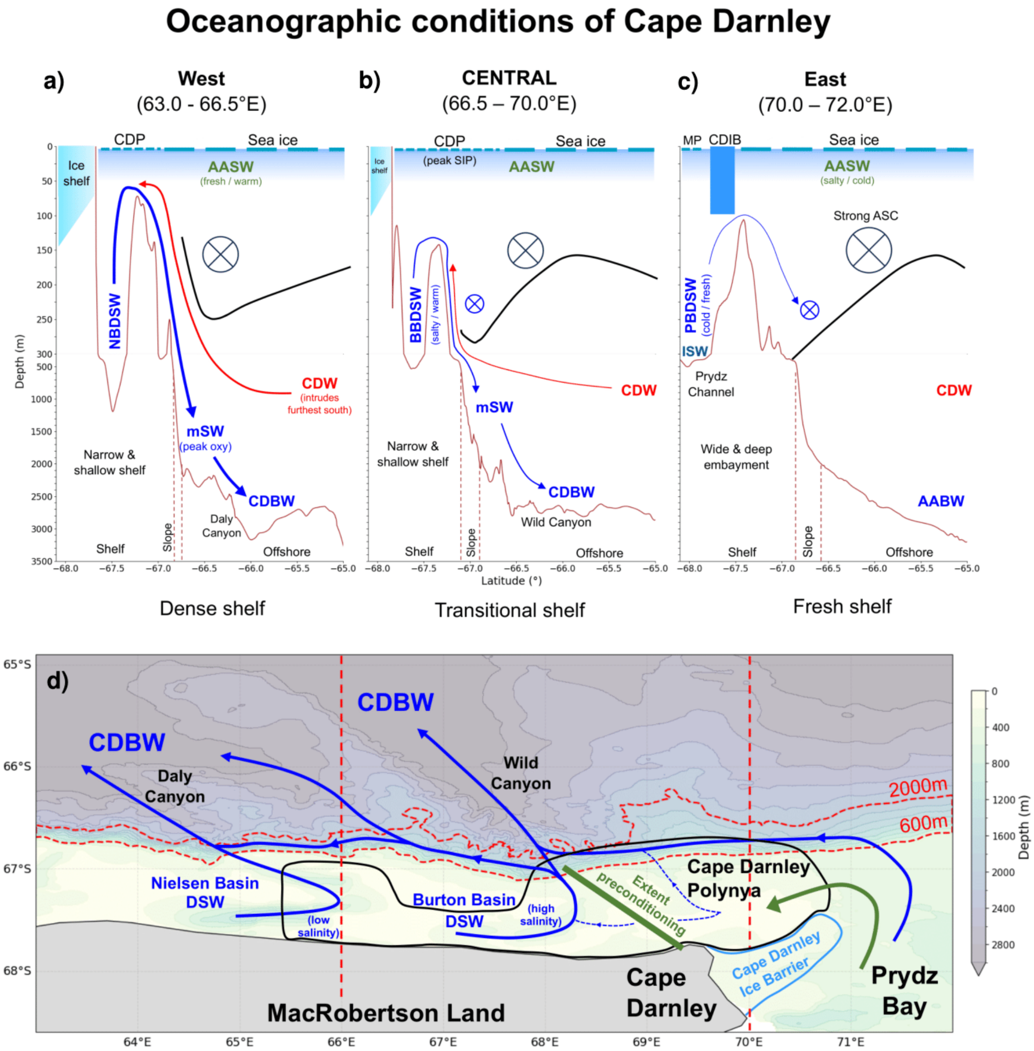


Figure 9: Schematic of Cape Darnley sectors (a - west, b - central, c - east) with bathymetry (brown), 28.00 kg/m$^3$ isoneutral (black), direction of Antarctic Slope Current (ASC) (black cross circle) and direction DSW slope flow (blue cross circle). Plan view (d) shows sectors, isobaths (600  2000 m – horizontal, dashed red lines), longitudinal split (vertical, dashed red lines) Cape Darnley Polynya (CDP - black), Cape Darnley Ice Barrier (CDIB - light blue), transport pathways of Dense Shelf Water (DSW) and Cape Darnley Bottom Water (CDBW) (solid dark blue), proposed DSW pathway of DSW from the north-east portion of the CDP (dashed dark blue), and extent of surface preconditioning from Prydz Bay (green). AASW = Antarctic Surface Water, mSW = modified shelf water, CDW = circumpolar deep water, AABW = Antarctic Bottom Water, PB = Prydz Bay, NB = Nielsen Basin, BB = Burton Basin, CDP = Cape Darnley Polynya, MP = Mackenzie Polynya

#### *5.2.4 Comparison of CDBW characteristics to other AABW formation regions*

The formation of AABW at Cape Darnley (CDBW) is unique compared to the Ross Sea, Weddell Sea and Adélie Land bottom water formation sites as it doesn't have a shelf basin where the DSW can accumulate and densify through the season. Instead we propose that the key mechanism for CDBW formation is the preconditioning of cold, salty surface waters from the eastern sector (Prydz Bay) which flows west on the shelf to ∼68.5°E and facilitates high sea ice formation within the Cape Darnley Polynya. Thus, the DSW formed at Cape Darnley reaches a critical density to overflow the sill, despite the absence of a shelf basin. We identify these conditions produce the highest absolute salinity compared to other AABW formation sites, with a maximum salinity of 35.15 g/kg (0.08 g/kg above that previously recorded 35.07 g/kg in this region; Ohshima et al. (2013)). We identify a high salinity variant exported through the Burton Basin (up to 35.15 g/kg) and down the Wild Canyon, and a low salinity variant exported through the Nielsen Basin (up to 34.85 g/kg) and down the Daly Canyon. More research is required to quantify the volume of export through these two export pathways in the Cape Darnley region. AABW is defined as having a neutral density of 28.27 kg/m$^3$ or greater (Orsi et al., 1999) and using this definition for the presence of bottom water, we propose that the CDBW has the warmest upper temperature boundary at 0.05°C. The main AABW formation mechanisms across the four formation sites are summarised and compared in Table 3.

Table 3: Comparison of four Antarctic Bottom Water formation sites using outcomes from this study and adapted from Budillon et al. (2011); Wang et al. (2012); G. D. Williams et al. (2010); Ohshima et al. (2013); G. D. Williams et al. (2008); Orsi & Wiederwohl (2009); Marsland et al. (2004); Tamura et al. (2008); Silvano et al. (2020); Foldvik et al. (2004); Gordon et al. (2015).

| | **Cape Darnley** | **Adélie** | **Ross** | **Weddell** |
|---|---|---|---|---|
| **Longitude** | ∼69°E | ∼145°E | ∼170°E | ∼60°W |
| **Blocking Ice Barrier** | Yes – Cape Darnley Ice Barrier | Yes – B-9b and Ninnis Glacier Tongue remnant icebergs | Yes – (only Terra Nova Polynya) Drygalski Ice Tongue | No |
| **Preconditioning from upstream** | Yes, Prydz Bay | No | No | No |
| **Large embayment** | No | Yes | Yes | Yes |
| **Shelf depth** | <400 m | <1000 m | <1000 m | <1000 m |
| **Polynya over shelf break** | Yes | No | No | No |
| **Polynya ice production ($km^3$/yr)** | 181 | 180 | 449.2 | 84.6 |
| **ISW impacting DSW** | Minimal | Minimal | Yes | Yes – biggest influence here |
| **High & low salinity DSW variant** | HSSW Wild Canyon LSSW Daly Canyon | HSSW Adélie Depression LSSW Mertz Depression | HSSW Drygalski Trough LSSW Joides Trough | HSSW From south-west LSSW Near Filchner depression & western shelf |
| **Max DSW absolute salinity observation (g/kg)** | 35.15 | 34.9 | 34.9 | 34.87 |
| **Upper conservative temperature bound of AABW (°C)** | <0.05 | <0 | <-0.1 | <-0.8 |
| **Percent contribution to global AABW** | 6–13% | 2–9% | 30–40% | 50–60% |

[1] Note: ISW = Ice Shelf Water; DSW = Dense Shelf Water; HSSW = High Salinity Shelf Water; LSSW = Low Salinity Shelf Water; AABW: Antarctic Bottom Water

### 5.3 Conclusions

Cape Darnley is a major contributor to global AABW, producing 6–13% of the total AABW formation. However it is the least studied AABW formation site due to its relatively recent discovery in 2013. Here we collate 40 years of oceanographic data available for this region and review the physical oceanography. We identified three distinct meridional sectors (east, central, west), with different oceanographic processes that influence the temperature and salinity characteristics of the DSW that is formed from the polynyas in this region. In comparison to other AABW formation sites, Cape Darnley has no large basin for DSW accumulation. Instead the primary driver of CDBW is high levels of sea ice production from the Cape Darnley Polynya and we found the westward movement of surface waters from Prydz Bay provides cold, salty surface waters to the central sector, to approximately 68.5°E, enhancing sea ice production in the north-east portion of the Cape Darnley Polynya.

We found two distinct DSW variants, a high salinity DSW observed in the Burton Basin and a lower salinity DSW in the Nielsen Basin. Smaller volumes of Burton Basin DSW are exported off shelf under a transitional shelf regime down the Wild Canyon, while larger volumes of Nielsen Basin DSW are exported offshore under a dense shelf regime via the Daly Canyon. This high salinity variant is the saltiest DSW (up to 35.15 g/kg) of all the AABW formation sites. The DSW is transformed to mSW and ultimately to CDBW at depths >1000 m and creates the warmest variant of AABW with an upper temperature bound of 0.05°C and an upper salinity bound of 34.845 g/kg. Collecting repeat transects on the shelf and enhancing sensors (e.g. adding oxygen to seal CTDs) will provide vital information to help determine export volumes, sources, and help to resolve slope and shelf processes at a higher resolution.

## Open Research Section

All sources and information about the raw shipboard CTD data can be found in Table 1. The marine mammal data were collected and made freely available by the International MEOP Consortium and the national programs that contribute to it (`http://www.meop.net`). The location and season of all raw data can be observed in Supp. Figure S1. The source code for the plots used in this study and the data product containing the raw data, gridded, and mean data can be found at 10.5281/zenodo.10976304.

**Acknowledgments**

This research was made possible and funded by ARC DP funding and a grant of sea time on the RV Investigator from the CSIRO Marine National Facility to Helen Bostock and Alix Post. The authors acknowledge support from the science team and crew onboard the RV Investigator IN2023_V01 for their support and advise in the early stages of this study. This research was supported by the use of the Australian Research Data Commons (ARDC) Nectar Research Cloud, a collaborative Australian research platform supported by the NCRIS-funded ARDC.

## References

Aoki, S., Ono, K., Hirano, D., & Tamura, T. (2020). Continuous winter oceanic profiling in the cape darnley polynya, east antarctica. *Journal of oceanography*, *76*(5), 365–372.

Bindoff, N., Rintoul, S., & Massom, R. (2000). Bottom water formation and polynyas in adelie land, antarctica. *Papers and proceedings of the Royal Society of Tasmania*, *133*(3), 51–56.

Blanckensee, S. N. (2024). *Siennaneve/cdobs: Cape darnley, east antarctica, antarctic bottom water data collation nc files.* Retrieved from `doi:10.5281/`

zenodo.10976304[Dataset]

Bourreau, L., Pauthenet, E., Le Ster, L., Picard, B., Portela, E., Sallée, J. B., ... Labrousse, S. (2023). First description of in situ chlorophyll fluorescence signal within east antarctic coastal polynyas during fall and winter. *Frontiers in Marine Science*, *10*.

Boyer, T. P., Baranova, O. K., Coleman, C., Garcia, H. E., Grodsky, A., Locarnini, R. A., ... Zweng, M. M. (2018). *Noaa atlas nesdis 87* (Tech. Rep.). World Ocean Database.

Budillon, G., Castagno, P., Aliani, S., Spezie, G., & Padman, L. (2011). Thermohaline variability and antarctic bottom water formation at the ross sea shelf break. *Deep-sea research. Part I, Oceanographic research papers*, *58*(10), 1002–1018.

Cougnon, E. A., Galton-Fenzi, B. K., Meijers, A. J. S., & Legrésy, B. (2013). Modeling interannual dense shelf water export in the region of the mertz glacier tongue (1992-2007): Modeling interannual dense shelf water. *Journal of geophysical research. Oceans*, *118*(10), 5858–5872.

Darelius, E., Daae, K., Dundas, V., Fer, I., Hellmer, H. H., Janout, M., ... Østerhus, S. (2023). Observational evidence for on-shelf heat transport driven by dense water export in the weddell sea. *Nature communications*, *14*(1), 1022–1022.

Dinniman, M. S., Asay-Davis, X. S., Galton-Fenzi, B. K., Holland, P. R., Jenkins, A., & Timmermann, R. (2016). Modeling ice shelf/ocean in antarctica a review. *Oceanography (Washington, D.C.)*, *29*(4), 144–153.

Fogwill, C. J., Phipps, S. J., Turney, C. S. M., & Golledge, N. R. (2015). Sensitivity of the southern ocean to enhanced regional antarctic ice sheet meltwater input. *Earth's future*, *3*(10), 317–329.

Foldvik, A., Gammelsrod, T., Osterhus, S., Fahrbach, E., Rohardt, G., Schroeder, M., ... Woodgate, R. A. (2004). Ice shelf water overflow and bottom water formation in the southern weddell sea. *Journal of Geophysical Research*, *109*(C2), C02015–n/a.

Fraser, A. D., Ohshima, K. I., Nihashi, S., Massom, R. A., Tamura, T., Nakata, K., ... Willmes, S. (2019). Landfast ice controls on sea-ice production in the cape darnley polynya: A case study. *Remote sensing of environment*, *233*, 111315.

Gao, L., Zu, Y., Guo, G., & Hou, S. (2022). Recent changes and distribution of the newly-formed cape darnley bottom water, east antarctica. *Deep-sea research. Part II, Topical studies in oceanography*, *201*, 105119.

GEBCO Compilation Group. (2023). *Gebco 2023 grid.* Retrieved 14-07-2023, from https://www.gebco.net/data_and_products/gridded_bathymetry_data/gebco_2023/[Dataset]

Gill, A. (1973). Circulation and bottom water production in the weddell sea. *Deep-sea research and oceanographic abstracts*, *20*(2), 111–140.

Gordon, A. L., Huber, B. A., & Busecke, J. (2015). Bottom water export from the western ross sea, 2007 through 2010. *Geophysical research letters*, *42*(13), 5387–5394.

Gunn, K. L., Rintoul, S. R., England, M. H., & Bowen, M. M. (2023). Recent reduced abyssal overturning and ventilation in the australian antarctic basin. *Nature climate change*, *13*(6), 537–544.

Guo, G., Gao, L., Shi, J., & Zu, Y. (2022). Wind-driven seasonal intrusion of modified circumpolar deep water onto the continental shelf in prydz bay, east antarctica. *Journal of geophysical research. Oceans*, *127*(12), n/a.

Herraiz-Borreguero, L., Church, J. A., Allison, I., Pena-Molino, B., Coleman, R., Tomczak, M., & Craven, M. (2016). Basal melt, seasonal water mass transformation, ocean current variability, and deep convection processes along the amery ice shelf calving front, east antarctica. *Journal of geophysical research. Oceans*, *121*(7), 4946–4965.

Herraiz-Borreguero, L., Coleman, R., Allison, I., Rintoul, S. R., Craven, M., &

Williams, G. D. (2015). Circulation of modified circumpolar deep water and basal melt beneath the amery ice shelf, east antarctica. *Journal of geophysical research. Oceans*, *120*(4), 3098–3112.

Huneke, W. G. C., Morrison, A. K., & Hogg, A. M. (2022). Spatial and subannual variability of the antarctic slope current in an eddying ocean–sea ice model. *Journal of physical oceanography*, *52*(3), 347–361.

IOC, SCOR and IAPSO. (2010). *The international thermodynamic equation of seawater – 2010: Calculation and use of thermodynamic properties.* Retrieved 05-07-2022, from `http://www.teos-10.org/`

Jacobs, S. S. (1991). On the nature and significance of the antarctic slope front. *Marine chemistry*, *35*(1), 9–24.

Johnson, G. C. (2008). Quantifying antarctic bottom water and north atlantic deep water volumes. *Journal of Geophysical Research*, *113*(C5), C05027–n/a.

Kitade, Y., Shimada, K., Tamura, T., Williams, G. D., Aoki, S., Fukamachi, Y., ... Ohshima, K. I. (2014). Antarctic bottom water production from the vincennes bay polynya, east antarctica. *Geophysical research letters*, *41*(10), 3528–3534.

Kusahara, K., Hasumi, H., & Tamura, T. (2010). Modeling sea ice production and dense shelf water formation in coastal polynyas around east antarctica. *Journal of Geophysical Research*, *115*(C10), n/a.

Marsland, S. J., Bindoff, N. L., Williams, G. D., & Budd, W. F. (2004). Modeling water mass formation in the mertz glacier polynya and adelie depression, east antarctica. *Journal of Geophysical Research*, *109*(C11), C11003–n/a.

McMahon, C. R., Hindell, M. A., Charrassin, J. B., Coleman, R., Guinet, C., Harcourt, R., ... Ribeiro, N. (2023). Southern ocean pinnipeds provide bathymetric insights on the east antarctic continental shelf. *Communications earth environment*, *4*(1), 266–10.

Meijers, A., Klocker, A., Bindoff, N., Williams, G., & Marsland, S. (2010). The circulation and water masses of the antarctic shelf and continental slope between 30 and 80 e. *Deep-sea research. Part II, Topical studies in oceanography*, *57*(9), 723–737.

MEOP. (2015). *Marine mammals exploring the oceans pole to pole.* Retrieved 15-09-2022, from `https://www.meop.net/index.html[Dataset]`

Mizuta, G., Fukamachi, Y., Simizu, D., Matsumura, Y., Kitade, Y., Hirano, D., ... Ohshima, K. I. (2021). Seasonal evolution of cape darnley bottom water revealed by mooring measurements. *Frontiers in Marine Science*, *8*.

Morrison, A. K., McC. Hogg, A., England, M. H., & Spence, P. (2020). Warm circumpolar deep water transport toward antarctica driven by local dense water export in canyons. *Science advances*, *6*(18), eaav2516–eaav2516.

National Institude of Polar Research. (2009). *Academic databases.* Retrieved 04-12-2023, from `https://scidbase.nipr.ac.jp/modules/metadata/index.php?content_id=259[Dataset]`

Nunes Vaz, R. A., & Lennon, G. W. (1996). Physical oceanography of the prydz bay region of antarctic waters. *Deep-sea research. Part I, Oceanographic research papers*, *43*(5), 603–641.

Ohashi, Y., Yamamoto-Kawai, M., Kusahara, K., Sasaki, K., & Ohshima, K. I. (2022). Age distribution of antarctic bottom water off cape darnley, east antarctica, estimated using chlorofluorocarbon and sulfur hexafluoride. *Scientific reports*, *12*(1), 8462–8462.

Ohshima, K. I., Fukamachi, Y., Ito, M., Nakata, K., Simizu, D., Ono, K., ... Tamura, T. (2022). Dominant frazil ice production in the cape darnley polynya leading to antarctic bottom water formation. *Science advances*, *8*(42), eadc9174–eadc9174.

Ohshima, K. I., Fukamachi, Y., Williams, G. D., Nihashi, S., Roquet, F., Kitade, Y., ... Wakatsuchi, M. (2013). Antarctic bottom water production by intense sea-ice

formation in the cape darnley polynya. *Nature geoscience*, *6*(3), 235–240.
Ohshima, K. I., Nihashi, S., & Iwamoto, K. (2016). Global view of sea-ice production in polynyas and its linkage to dense/bottom water formation. *Geoscience Letters*, *3*(1), 1.
Orsi, A. H., Johnson, G. C., & Bullister, J. P. (1999). Circulation, mixing, and production of antarctic bottom water. *Progress in oceanography*, *43*(1), 55–109.
Orsi, A. H., Smethie, W. M., & Bullister, J. L. (2002). On the total input of antarctic waters to the deep ocean; a preliminary estimate from chlorofluorocarbon measurements. *Journal of Geophysical Research*, *107*(C8), 31-1–31-14.
Orsi, A. H., & Wiederwohl, C. L. (2009). A recount of ross sea waters. *Deep-sea research. Part II, Topical studies in oceanography*, *56*(13), 778–795.
Portela, E., Rintoul, S. R., Bestley, S., Herraiz-Borreguero, L., Wijk, E., McMahon, C. R., ... Hindell, M. (2021). Seasonal transformation and spatial variability of water masses within mackenzie polynya, prydz bay. *Journal of geophysical research. Oceans*, *126*(12), n/a.
Portela, E., Rintoul, S. R., Herraiz-Borreguero, L., Roquet, F., Bestley, S., Wijk, E., ... Hindell, M. A. (2022). Controls on dense shelf water formation in four east antarctic polynyas. *Journal of geophysical research. Oceans*, *127*(12), n/a.
Sea-Bird Scientific. (2023). *Sbe 9plus ctd.* Retrieved 04-12-2023, from `https://www.seabird.com/asset-get.download.jsa?id=54663149001`
Sea-Bird Scientific. (2024). *Sbe 911plus ctd.* Retrieved 04-12-2023, from `https://www.seabird.com/sbe-911plus-ctd/product?id=60761421595`
Shapiro, G. I., Huthnance, J. M., & Ivanov, V. V. (2003). Dense water cascading off the continental shelf. *Journal of Geophysical Research*, *108*(C12), 3390–n/a.
Silvano, A., Foppert, A., & Macdonald, A. M. (2020). Recent recovery of antarctic bottom water formation in the ross sea driven by climate anomalies. *Nature geoscience*, *13*(12), 780–786.
Tamura, T., Ohshima, K. I., Fraser, A. D., & Williams, G. D. (2016). Sea ice production variability in antarctic coastal polynyas. *Journal of geophysical research. Oceans*, *121*(5), 2967–2979.
Tamura, T., Ohshima, K. I., & Nihashi, S. (2008). Mapping of sea ice production for antarctic coastal polynyas: Mapping of sea ice production. *Geophysical research letters*, *35*, n/a.
Thompson, A. F., Stewart, A. L., Spence, P., & Heywood, K. J. (2018). The antarctic slope current in a changing climate. *Reviews of geophysics (1985)*, *56*(4), 741–770.
Wang, Q., Danilov, S., Fahrbach, E., Schröter, J., & Jung, T. (2012). On the impact of wind forcing on the seasonal variability of weddell sea bottom water transport. *Geophysical research letters*, *39*(6), n/a.
Whitworth, T., Orsi, A. H., Kim, S., Nowlin, W. D., & Locarnini, R. A. (1985). Water masses and mixing near the antarctic slope front. In *Ocean, ice, and atmosphere: Interactions at the antarctic continental margin* (pp. 1–27). Washington, D. C: American Geophysical Union.
Williams, G., Nicol, S., Aoki, S., Meijers, A., Bindoff, N., Iijima, Y., ... Klocker, A. (2010). Surface oceanography of broke-west, along the antarctic margin of the south-west indian ocean ( 30 – 80 e ). *Deep-sea research. Part II, Topical studies in oceanography*, *57*(9), 738–757.
Williams, G. D., Aoki, S., Jacobs, S. S., Rintoul, S. R., Tamura, T., & Bindoff, N. L. (2010). Antarctic bottom water from the adelie and george v land coast, east antarctica (140-149 degrees e). *Journal of Geophysical Research*, *115*(C4), n/a.
Williams, G. D., Bindoff, N. L., Marsland, S. J., & Rintoul, S. R. (2008). Formation and export of dense shelf water from the adelie depression, east antarctica. *Journal of Geophysical Research*, *113*(C4), C04039–n/a.
Williams, G. D., Herraiz-Borreguero, L., Roquet, F., Tamura, T., Ohshima, K. I.,

Fukamachi, Y., … Hindell, M. (2016). The suppression of antarctic bottom water formation by melting ice shelves in prydz bay. *Nature communications*, *7*(1), 12577–12577.

# A review of the oceanography and Antarctic Bottom Water formation offshore Cape Darnley, East Antarctica

**Sienna N. Blanckensee[1], David E. Gwyther[1], Ben K. Galton-Fenzi [2], Kathryn L. Gunn [3], Laura Herraiz-Borreguero[4],[5], Kay I. Ohshima [6], Esther Portela Rodriguez[7], Alexandra L. Post [8], Helen C. Bostock[1]**

[1]School of the Environment, The University of Queensland, Australia
[2]Australian Antarctic Division, Hobart, Tasmania, Australia
[3]School of Ocean and Earth Science, University of Southampton, Southampton, UK
[4]CSIRO Environment, Hobart, Tas, 7004, Australia
[5]Australian Antarctic Partnership Program, Hobart, Tas, 7004, Australia
[6]Institute of Low Temperature Science, Hokkaido University, Japan
[7]Laboratoire d'Oceanographie Physique et Spatiale (LOPS), University Brest, CNRS, IRD, Ifremer, Plouzane, France
[8]Geoscience Australia, Canberra, Australia

**Key Points:**

- Water masses and processes in Prydz Bay precondition and influence the characteristics of the DSW formation in Cape Darnley to ∼68.5°E
- A high and low salinity variant of DSW is exported from Cape Darnley, observing the highest maximum salinity of all AABW formation sites.
- Cape Darnley Bottom Water has the warmest upper bound temperature of the four sources of AABW.

Corresponding author: Sienna Blanckensee, `s.blanckensee@uq.net.au`

**Abstract**

Antarctic Bottom Water (AABW) is the densest water mass in the world and drives the lower limb of the global thermohaline circulation. AABW is formed in only four regions around Antarctica and Cape Darnley, East Antarctica, is the most recently discovered formation region. Here, we compile 40 years of oceanographic data for this region to provide the climatological oceanographic conditions, and review the water mass properties and their role in AABW formation. We split the region into three sectors (East, Central and West) and identified the main water masses, current regimes and their influence on the formation of Cape Darnley Bottom Water (CDBW). In the eastern sector, Prydz Bay, the formation of Ice Shelf Water preconditions the water (cold and fresh) that flows into the central sector to $\sim$68.5°E, enhancing sea ice production in Cape Darnley Polynya. This produces a high salinity variant of DSW (up to 35.15 g/kg) DSW that we coin Burton Basin DSW. In contrast, the western sector of the Cape Darnley Polynya produces a low salinity variant (up to 34.85 g/kg) we coin Nielsen Basin DSW. The resultant combined CDBW is the warmest (upper temperature bound of 0.05°C) AABW formed around Antarctica with an upper bound salinity of $\sim$34.845 g/kg. Our findings will contribute to planning future observing systems at Cape Darnley, determining the role CDBW plays in our global oceanic and climate systems, and modelling past and future climate scenarios.

## Plain Language Summary

Around Antarctica, there are four areas where very high sea ice production makes water dense enough to sink to the sea floor. This water is called Antarctic Bottom Water and plays a vital role in deep water circulation and moving cold water towards the equator, therefore regulating global climate. Cape Darnley, in East Antarctica, is the most recently discovered of these four areas and hence has been less studied. Cape Darnley Bottom Water is unique as it forms via slightly different processes to the other three formation sites. In this study, we have pulled together all the data in the region over a 40-year period for the first time. We found that very cold water flows into the region from upstream, making conditions ideal for very high sea ice production at Cape Darnley. This forms a higher and lower salinity dense water mass that flows down different pathways before combining to become Cape Darnley Bottom Water, which is warmer and saltier than the other three areas. These findings are critical for planning future data collection, understanding the impact this site has on the global ocean circulation, and how climate change could impact Antarctic Bottom Water in the future.

## 1 Introduction

Antarctic Bottom Water (AABW) is the densest water mass in the globe due to its high salinity and cold temperatures. It occupies the abyssal layers of the ocean and accounts for 30-40% of oceanic volume. AABW supplies the lower limb of the meridional overturning circulation (Cougnon et al., 2013; Johnson, 2008) and it plays a key role in the climate system and biogeochemical cycles by transporting cold, salty, oxygen and carbon-rich waters to the deep ocean (Bindoff et al., 2000; Ohshima et al., 2013; Orsi et al., 1999; Shapiro et al., 2003). Over the last 50 years, AABW has experienced freshening, warming, and significant contraction, which threatens this major global circulation (G. D. Williams et al., 2010; Tamura et al., 2008; Fogwill et al., 2015).

AABW forms at four locations around Antarctica: the Weddell Sea, Ross Sea, Adélie Land (Cougnon et al., 2013), and Cape Darnley, most recently discovered in 2013 by Ohshima et al. (2013). Despite a number of studies in the Cape Darnley region (Mizuta et al., 2021; Gao et al., 2022; Aoki et al., 2020; Ohashi et al., 2022; Fraser et al., 2019; Ohshima et al., 2013, 2022) and a growing hydrographic dataset since its discovery, we are yet to determine the mean state of the region and to understand the role each water mass plays in Cape Darnley Bottom Water (CDBW) formation. Here we compile 40 years of oceanographic data to provide an ocean climatology of Cape Darnley for the first time. Our work provides an improved understanding of the characteristics of the Dense Shelf Water (DSW) that forms in the region, which is the precursor to CDBW.

## 2 Oceanographic Context

The DSW mass formed over the continental shelf of Antarctica is the precursor for AABW (Kusahara et al., 2010; Kitade et al., 2014; Ohshima et al., 2013; Cougnon et al., 2013; G. D. Williams et al., 2010). DSW formation requires an active polynya where continuous sea ice production results in brine rejection and significantly increases the density of the water column beneath (Kusahara et al., 2010; Kitade et al., 2014; Ohshima et al., 2013; Cougnon et al., 2013; G. D. Williams et al., 2010). However, the density and formation of DSW is also controlled by other water masses, regional circulation, and shelf geography (Portela et al., 2022).

AABW formation occurs at sites around the Antarctic margin that possess the necessary pre-existing oceanographic conditions and an active polynya. The Ross Sea polynyas exhibit the highest sea ice production (449.2 $km^3$/yr), while the Cape Darnley and Adélie Land polynyas contribute 181 $km^3$/yr and 180 $km^3$/yr respectively, with the Weddell Polynya exhibiting the smallest production rate at 84.6 $km^3$/yr (Tamura et al., 2008; G. D. Williams et al., 2010). However, sea ice production rates are not directly correlated with percentage contribution to global AABW, with the Weddell Sea and Ross Sea contributing 50–60% and 30–40% of the total AABW respectively (Orsi et al., 2002, 1999; Foldvik et al., 2004; Ohshima et al., 2016). The remaining AABW is sourced from East Antarctica, with Cape Darnley contributing 6–13% and Adélie Land contributing 2–9% (Ohshima et al., 2013; Orsi et al., 2002; G. D. Williams et al., 2008).

In the Ross Sea, Weddell Sea and Adélie Land regions, DSW forming polynyas occur over wide and deep coastal embayments, with the polynya typically inland from the continental shelf break (Orsi & Wiederwohl, 2009; Silvano et al., 2020; Foldvik et al., 2004; Wang et al., 2012; Marsland et al., 2004; G. D. Williams et al., 2008). For example, the Ross Sea polynya is 400 km from the shelf break (G. D. Williams et al., 2010). This position and bathymetric conditions play a critical role allowing DSW to accumulate and reach a sufficient density over time, prior to export down the slope to form AABW (G. D. Williams et al., 2016; Foldvik et al., 2004; Ohshima et al., 2016).

DSW formation is also influenced by water masses and ocean circulation north of the continental shelf. The intrusion of warm, salty, offshore Circumpolar Deep Waters (CDW) onto the shelf can also be impacted by slope processes such as the presence of the Antarctic Slope Current (ASC), a strong, narrow current along the continental slope. The ASC exhibits as strong temperature gradient, and is also coined the Antarctic Slope Front (ASF), which acts as a barrier between the open ocean and shelf waters (Thompson et al., 2018; Huneke et al., 2022; G. Williams et al., 2010). Where DSW is exported over the continental shelf break, the isoneutrals in this front shoal, creating a "V" shape (Marsland et al., 2004). This is known as a dense shelf regime, and allows for the intrusion of the warm (~1°C) and salty CDW onto the continental shelf (Dinniman et al., 2016; Bindoff et al., 2000). The three AABW formation regions also observe an intrustion of CDW via a large, clockwise circulation around the embayments. Once on the shelf, CDW mixes with shelf water masses to become modified CDW (mCDW) (Cougnon et al., 2013). This mixing of water masses influencing the shelf water properties and local processes that lead to DSW formation and export in the region (e.g. driving increased Ice Shelf Water (ISW) formation) (Orsi & Wiederwohl, 2009; Foldvik et al., 2004; G. D. Williams et al., 2010).

As a result of variations in the processes above, each of the four regions produce DSW with slightly different characteristics. Cape Darnley creates the highest absolute salinity DSW reaching up to 35.07 g/kg, with the Ross Sea and Adélie Land DSW both exhibiting salinities of 34.9 g/kg (Silvano et al., 2020; G. D. Williams et al., 2010; Ohshima et al., 2013). The freshest DSW is exhibited in the Weddell Sea, with a salinity of 34.87 g/kg, due to the presence of cold and fresh ISW from the Filchner Depression and the western shelf (Foldvik et al., 2004; Darelius et al., 2023).

Once DSW has formed, and is of sufficient density, it flows down the continental slope via export pathways (down canyons or as cascading plumes, eddies, or gravity currents). G. D. Williams et al. (2010) found that calculating a quantitative critical density for DSW that leads to AABW is not plausible as it varies greatly by region, within regions, and interannually. Within each region, there is evidence for a split in DSW export exhibiting a high salinity and low salinity variant (Wang et al., 2012; G. D. Williams et al., 2010).

The exported DSW is altered by the entrainment of ambient offshore water masses, primarily CDW, creating a warmer, less dense, modified Shelf Water (mSW) on the slope. As mSW continues to descend, it entrains more CDW, eventually becoming AABW, defined as having a neutral density of 28.27 kg/m$^3$ or greater (Bindoff et al., 2000; Ohshima et al., 2013). On the sea floor, the thermobaric effect causes temperature to become the dominant component of the AABW neutral density (G. D. Williams et al., 2010). For each formation location the AABW temperature differs depending on the formation process. For example the upper temperature boundary for this density gradient is the lowest in the Weddell Sea region with a conservative temperature of -0.7°C, due to the role of ISW (Wang et al., 2012). The Ross Sea and Adélie Land have similar upper boundary temperatures of -0.1°C and 0°C respectively (Budillon et al., 2011; G. D. Williams et al., 2010).

### 2.1 Cape Darnley Bottom Water Formation

Cape Darnley is located in East Antarctica, west of the Prydz Bay and Amery Ice Shelf, ranging between 64 to 69.5°E. The cape and a grounded ice barrier (Cape Darnley Ice Barrier) block the westward movement of sea ice, creating ideal conditions for the Cape Darnley Polynya to form over the MacRoberston Land continental shelf. However, the region was initially dismissed as a potential region for AABW formation as this area does not have a large embayment and basin like the Ross, Weddell and Adélie regions, instead it has a shallow, narrow continental shelf ($\sim$90 km), with a large portion of the polynya lying directly over the shelf break and upper slope (Figure 1)(Ohshima et al., 2013, 2016).

The discovery of DSW export from the Cape Darnley Polynya highlighted that the criteria previously believed necessary for DSW and AABW formation may not apply to all regions. Despite the narrow shelf, the DSW formed here achieves the required density to form AABW, attributed to the high sea ice production in the polynya (Ohshima et al., 2013, 2016). The Cape Darnley Polynya has the smallest area (13000 $\pm$ 1600 km$^2$) of the four AABW polynya sites, however, it has the second highest sea ice production rate (182 $\pm$ 23 km$^3$/yr) (Tamura et al., 2016). A recent study by Ohshima et al. (2022) also suggests that frazil ice up to 80 m below sea level dominates in the polynya. This further facilitates efficient sea ice production and prevents thick sea ice from forming (Ohshima et al., 2022). The DSW in this region reaches a minimum salinity in May, and becomes the dominant water mass on the shelf between August and October (Portela et al., 2022). However, DSW seasonality in the Cape Darnley region is still difficult to assess due to limited sampling and data (Portela et al., 2022).

To the east of Cape Darnley, Prydz Bay was initially thought to be a good candidate for a forth region of AABW formation as it contains three active polynyas (Mackenzie, Davis, and Barrier). The DSW formed in Prydz Bay does not reach sufficient density for export due to mixing processes with ISW from the Amery Ice Shelf (G. D. Williams et al., 2016; Cougnon et al., 2013; Ohshima et al., 2013; Mizuta et al., 2021). However, the westward flow of cooler water masses play an important role in preconditioning the Cape Darnley region shelf waters. It is likely that Prydz Bay DSW flows westward along the slope after descending the Prydz Channel (Nunes Vaz & Lennon, 1996; G. D. Williams et al., 2016). However, recent studies by Portela et al. (2021) conflict with this, suggesting DSW formed in Prydz Bay flows east due to gravity driven flows. Despite the contested extent of DSW preconditioning, the adjacent Prydz Bay region plays an important role in prescribing the water mass properties on the Cape Darnley shelf.

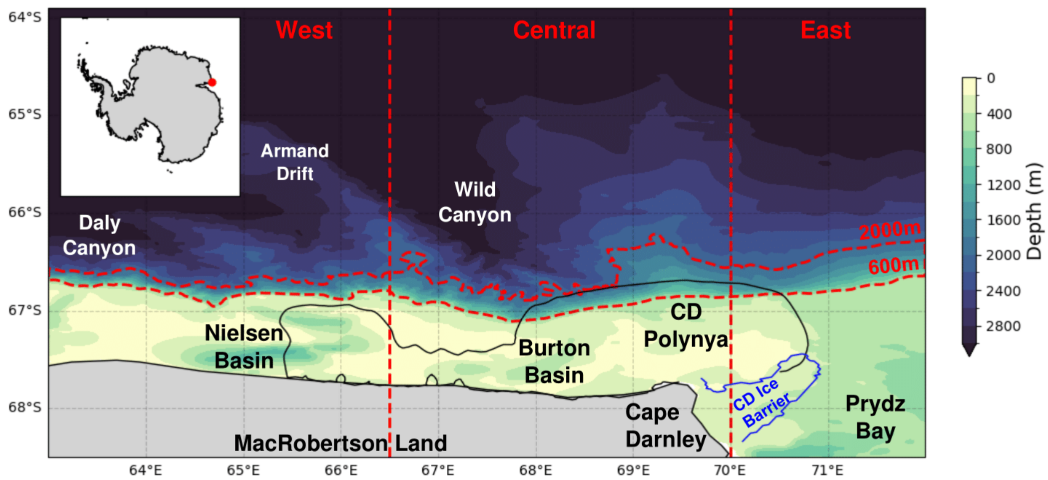


Figure 1: Cape Darnley study site with sea floor bathymetry.The black solid line shows the Cape Darnley polynya and the blue solid line shows the location of the Cape Darnley Ice Barrier (defined in section 3.0). The red dashed lines indicate the boundaries for the nine regions (defined in section 3.1) at the 600 m & 2000 m isobaths, 66.5°E and 70°E.

DSW formed in Cape Darnley is exported via the Wild and Daly Canyons. It descends to greater depths with the aid of thermobaricity and the steep continental slope to form CDBW (Ohshima et al., 2013). This steep slope at Cape Darnley is another key difference in the region, theorised to allow DSW to descend with less modification from ambient water masses, preventing the need for accumulation within a shelf basin (G. D. Williams et al., 2010). CDBW contributes 6-13% (2.13 Sv) of total AABW (Kusahara et al., 2010; Ohshima et al., 2013). Many studies have been conducted on CDBW since its discovery (Ohshima et al., 2013; Herraiz-Borreguero et al., 2015; Tamura et al., 2016; G. D. Williams et al., 2016; Fraser et al., 2019; Aoki et al., 2020; Gao et al., 2022; Guo et al., 2022; Ohashi et al., 2022; Ohshima et al., 2022; Portela et al., 2022; Bourreau et al., 2023). However, most of these studies focus on one aspect of the region, or use data with limited spatial or temporal resolution. In this paper we compile all the available hydrographic data from CTD, autonomous float and seal CTD over the last 40 years to provide the first ocean climatology of the Cape Darnley and western Prydz Bay region and new insights into the formation of DSW and AABW in this region. Understanding the current oceanic conditions at Cape Darnley is vital for monitoring and modelling experiments to assess the role climate change is having and will have on this system in the future.

## 3 Oceanographic data & Methodology

For this study, data within the Cape Darnley and western Prydz Bay region (defined as 65–68.5°S and 63–73°E) were collated over the past 40 years. This included data from ships, autonomous floats and instrumented southern elephant seals (*Mirounga leonina*; see Supp. Figure S1). All data sets were converted to TEOS-10 standards (i.e. absolute salinity, conservative temperature and neutral density) for comparison (IOC, SCOR and IAPSO, 2010). The resultant data product can be found at `10.5281/zenodo.10976304` (Blanckensee, 2024).

The different sources and methods of data collection have varying levels of instrument uncertainty (see Table 1). These datasets have all undergone post-processing before being released publicly (McMahon et al., 2023; Boyer et al., 2018; Ohashi et al., 2022). Nevertheless, further quality control was manually completed during the collation process. We removed data that exceeds reasonable bounds of temperature, salinity and oxygen (> 3 standard deviations from mean), which was primarily present in older ship datasets. Despite the inherent uncertainty in seal measurements, our analysis revealed a high degree of agreement between the seal dataset and the data obtained from ships and floats, as depicted in Supp. Figure S2. However, seal data does have an extra uncertainty in spatial location, with a median error of 3.2 km (McMahon et al., 2023). In order to take into account this spatial uncertainty, we chose to make our gridded analysis cells greater than this distance (0.1° by 0.1°).

An added layer of uncertainty in this combined ship, float and seal data set is the temporal variability resulting from collation of multi-year and -seasonal data into a single dataset. The variability introduced through combining multiple seasons into a single dataset can be observed in Figure 4 which displays data 0.5 standard deviations either side of the mean. The surface waters exhibit the greatest seasonality and hence greater variability, owing to their direct interaction with the atmosphere. However, a seasonal analysis of this region has previously been conducted by Portela et al. (2021) and the focus of this paper lies primarily on intermediate and bottom waters. Consequently, all seal data was included to increase the spatial coverage of the region. The collated dataset is also strongly biased to the last 15 years, as there was limited data collected prior to this time.

Table 1: Overview of data sources, ranges and measurement error (Ohashi et al., 2022; Boyer et al., 2018; Sea-Bird Scientific, 2023, 2024; National Institute of Polar Research, 2009; McMahon et al., 2023; MEOP, 2015)

| **Type** | **Years** | **Range** | | | **Data source** | **Measurement error** | | | |
|---|---|---|---|---|---|---|---|---|---|
| | | **Spatial** | **Temporal** | **Depth** | | **Salt (S·m-1)** | **Oxy (%)** | **Press** | **Temp (°C)** |
| Ships | 1981 – 2023 | Shelf (limited), slope & offshore | Primarily summer | Sea floor | WOD, AAD, CCHDO, RDA, NIPR | 0.0002 – 0.003 | 2 | 0.015 – 0.08% FS | 0.001 – 0.005 |
| Floats | 2009 – 2023 | Slope & offshore | All seasons | Core <2000m, Deep <4000m | WOD | 0.0005 – 0.001 | 2 – 5 | 2.4db | 0.002 |
| Seals | 2011 – 2019 | Shelf (primarily), slope & offshore | | <1600m | MEOP | 0.003 | - | 0.015% FS | 0.03 |

[1] median locational error seal data = 3.2 km

We sourced gridded bathymetry data from GEBCO v2023 (GEBCO Compilation Group, 2023). The fast ice and sea ice production contour outlining the Cape Darnley Polynya position was calculated from Tamura et al. (2016) product. The polynya contour delineates the 60 W/m$^2$ annual mean ocean heat loss (based on sea ice production contours used in Ohshima et al. (2013) and G. D. Williams et al. (2016)) and the fast ice boundary represents where ice is present for 95% of year (Tamura et al., 2016) product.

### 3.1 Analysis techniques

Water masses were first classified into three layers based on neutral density definitions previously identified by Orsi et al. (1999): surface, intermediate, bottom (<28.00, 28.00–28.27, >28.27 kg/m$^3$) (see isoneutrals in Figure 2). Depth, salinity and temperature conditions were then used to further classify the water masses based on previous studies of hydrographic characteristics from around East Antarctica (Herraiz-Borreguero et al., 2015, 2016; G. D. Williams et al., 2016; Orsi & Wiederwohl, 2009; Portela et al., 2021).

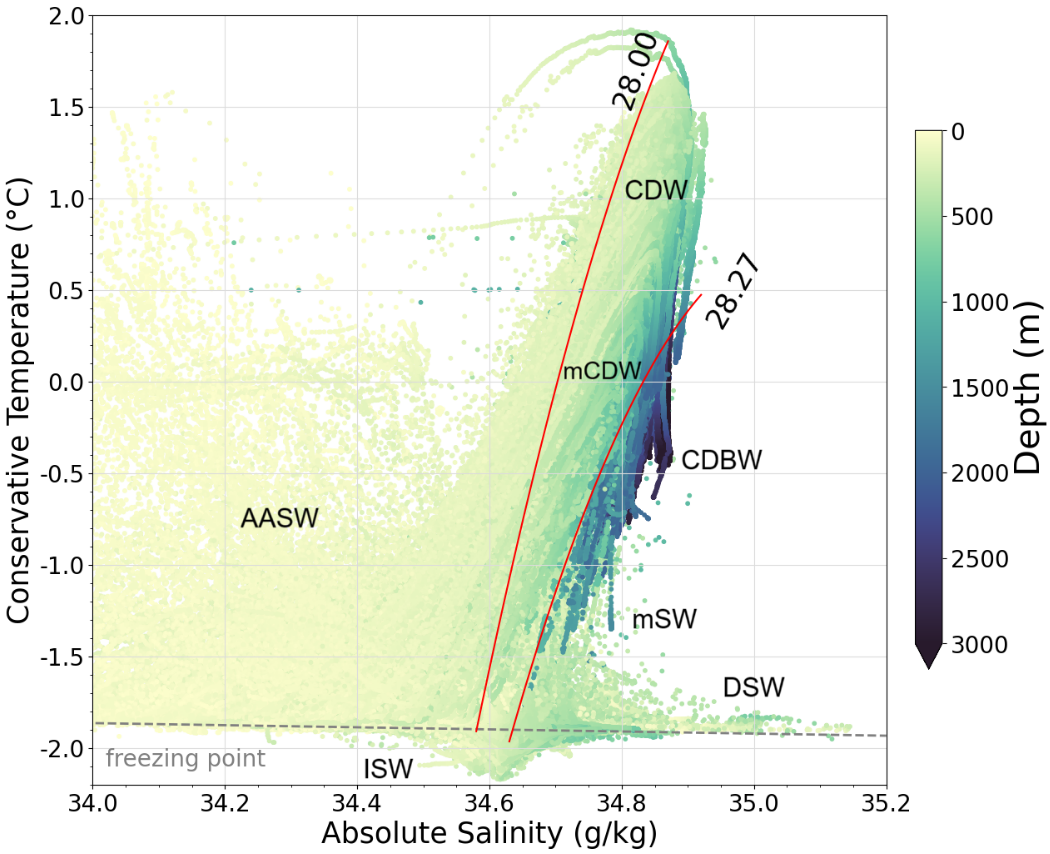


Figure 2: All data sources (ship, autonomous float & seal) in conservative temperature - absolute salinity space coloured by depth. The surface freezing point is represented by the gray dashed line and the 28.00 & 28.27 kg/m$^3$ neutral density lines are in red (see Supp Figure S2 for split in data between, ships, autonomous floats & seals).

The gridded spatial plots provide another insight into the region. For each individual cast, the mean absolute salinity and conservative temperature value was calculated for each density layer. The thickness of this layer was determined using the upper and lower depth values that fall within the density layer. The ship and float datasets have similar depth resolution (every 1–2 m). However, the depth resolution of seals varies with depth (i.e. 2.5 m for depths between 2.5–35 m; up to 25.0 m for depths between 420–1500 m). Although this may introduce slight discrepancies in the calculations due to its varied bin sizes, the dataset provides valuable insights into the shallower waters (<1000 m) on shelf and slope regions where there is limited CTD and float data. Then, to remove bias through over-plotting of co-located data, a 0.1° by 0.1° grid was created, with the mean of all points that fall within a cell displayed in Figures 5, 6 and 7 where each step represents 1/8th of the data points. Due to the data scarcity in this region, we have not excluded any grid cells based on a minimum data count to provide a more complete oceanographic representation of the region.

From this gridded analysis and bathymetry patterns, data was then partitioned into nine key regions for temperature-salinity and mean analysis. To capture shelf, slope and offshore processes, three zonal bands were identified: **shelf (<600 m depth)**, **slope (between 600–2000 m depth)** and **off-shore (north >2000 m depth)**. Then, to capture water mass changes along the coastline, three meridional bands were identified: **east – 70-72°** (western Prydz Bay / east of Cape Darnley), **central – 66.5-70°E** (highest sea ice production in the Cape Darnley Polynya and over the Burton Basin), and **west – 63-66.5°E** (lowest sea ice production in the Cape Darnley Polynya and over the Nielsen Basin).

To develop latitudinal depth transects, we identified the most recent offshore shipboard CTD transects within each meridional sector at 65°E, 68°E, and 70°E. These were then extended on to slope and shelf using any data source (ship, float, or seal) that fell along these longitudinal lines (excluding winter to minimise seasonal variation). Data were then linearly interpolated between points for spatial coherence.

# 4 Results

The following results have been partitioned into shelf, slope and offshore processes as each latitudinal band has distinct characteristics. These are then split into the surface, intermediate and bottom water masses, which are also discussed by the meridional sector location (east, central, and west).

## 4.1 SHELF (bathymetry <600 m)

### *4.1.1 Surface water masses ($y^n$ < 28.00 kg/m$^3$)*

On the continental shelf, AASWs have high variability (Figure 3g–3i) with temperatures ranging from -1.95°C to ∼1.0°C, and salinities ranging from 32 to 34.7 g/kg. East of Cape Darnley in the upper ∼200 m, AASW temperatures are the coldest (sitting along the surface freezing point of -1.95°C) and saltiest (∼0.4 g/kg higher than the sectors east of Cape Darnley) (Figure 4g & 4h). In the eastern sector, oxygen content also peaks (320 < O < 360 $\mu$mol/L) (Figure 4i). This cold (-1.95 < $\theta$ < -1.38 °C) and salty (34.3 < S_A < 34.72 g/kg) AASW is also evident in Figure 5a & 5b. Here, AASW has a thickness of 0 to ∼191 m, with the thinnest AASW east of the 71°E (Figure 5c). There is an isolated patch of thick AASW between 70–70.8°E and south of 68°S, with a thick (85 < T < 191 m), narrow, layer flowing along the 400 m isobath along the Prydz Channel to the edge of the slope.

Moving to the west the coldest (-1.95 < $\theta$ < -1.58 °C) and saltiest (34.42 < S_A < 34.72 g/kg) waters within the Cape Darnley Polynya are present in its north-east portion, similar to that in Prydz Bay (Figure 5). However, there is a sharp gradient in temperature and salinity along a line from (67.5°S, 68°E) to (67.8°S, 69.2°E). South-west of this line waters in the Cape Darnley Polynya are fresher (32.04 < S_A < 34.37 g/kg) and warmer (>-1.58°C). Overall, the central sector AASW exhibits the lowest oxygen content (260 < O < 330 $\mu$mol/L) (Figure 4i). Transitioning into the western sector, sea ice production in the Cape Darnley Polynya is lower than the central sector (Ohshima et al., 2013) and AASW gradually thickens (0 < T < 685 m), becomes fresher (33.95 < S_A < 34.65 g/kg), and warmer (-1.7 < $\theta$ < -1.3 °C) (Figure 4g – h & 5). There are also two thick (150 < T < 290 m), narrow, branches of AASW overlying the Nielsen and Burton Basins (Figure 5).

### *4.1.2 Intermediate water masses (28.00 < $y^n$ < 28.27 kg/m$^3$)*

On the shelf, water that falls into the intermediate density class is either mCDW, or falls along the mixing line between AASW and DSW. A lower temperature bound for mCDW has previously been defined as 0.1°C above the surface freezing point, but water along the mixing line can also exceed this temperature threshold (Portela et al., 2021). In this study, to differentiate mCDW and water along the mixing line, we use a lower temperature bound of approximately -1.2°C for mCDW. This temperature bound was determined from a discernible curve in the temperature-salinity plot that marks the transition from AASW to DSW, with an inflection point at approximately -1.2°C (Figure 3g–3i). Water parcels warmer than this threshold exhibit characteristic mCDW properties (warmer and saltier with mid range depths).

In the eastern sector, this intermediate layer is the thickest of the meridional regions (18 < T < 197 m) (Figure 6c). These intermediate waters exhibit lower temperatures (-1.95 < $\theta$ <-1.59°C) and sit along the mixing line with the thickest waters found directly east of the Cape Darnley Ice Barrier. A small amount of mCDW is found just south of the 600 m isobath line at approximately 67.1°S, with temperatures between -1.59 and -0.27°C (Figure 6).

West of 69°E, this intermediate layer sits below a depth of ~150 m and thins rapidly polewards towards the coastline (from 591 m to <18m). mCDW intrudes onto the shelf via the Nielsen and Burton Basins where there is a relatively thick (18 < T < 98 m) layer of warmer (-1.59 < $\theta$ < -0.27 °C) and saltier (34.64 < S_A < 34.74 g/kg) water which intrudes as far south as 67.4°S (Figure 6).

#### *4.1.3 Bottom water masses ($y^n$ > 28.27 kg/m$^3$)*

The bottom density layer principally captures DSW, which is present as a thin (<122 m) layer across the entire shelf (Figure 7). It exhibits temperatures near the surface freezing point (-1.95 < $\theta$ < -1.85 °C) and salinities >34.65 g/kg (Figure 3g–3i). The thickest (> 122 m) and largest volumes of DSW are found in the Nielsen Basin, Burton Basin, directly north of Cape Darnley and in Prydz Bay to the east (Figure 7c).

In the eastern sector, Prydz Bay DSW is the coldest (-2.16 < $\theta$ < -0.72 °C), freshest (34.62 < S_A < 34.81 g/kg) (Figure 3g & 3h) and most oxygenated (~320 $\mu$mol/L) (Figure 4i). However, ISW is also present within this density layer in the eastern sector as indicated by temperatures below the surface freezing point (-2.15 < $\theta$ < -1.95°C) and low salinities ( 32.51 < S_A < 34.62 g/kg) in front of the Amery Ice Shelf (Figure 3g–3i & Supp. Figure S3).

In the central shelf sector, DSW is the warmest (-1.6 < $\theta$ < -1.0 °C) and saltiest (up to 34.9 g/kg) (Figure 4g–4h & 7). This sector also records the highest singular salinity measurement, reaching 35.15 g/kg (Figure 3h). This salty DSW is found along the coastline and follows the Burton Basin towards the shelf break. Oxygen in this sector is the lowest of the three shelf sectors, reaching a minimum of 215 $\mu$mol/L (Figure 4i).

The western sector DSW is, on average, slightly cooler (-1.95 < $\theta$ < -1.5 °C), and fresher (up to 34.85 g/kg) in comparison to the central sector. This DSW can be observed around 65°E at the base of the Nielsen Basin at depths between approximately 400–1000 m (Figure 4g & 4h). Oxygen content in this sector falls between the east and central sectors (290 < O < 300 $\mu$mol/L (Figure 4i).

### 4.2 SLOPE (bathymetry 600–2000 m)

#### *4.2.1 Surface water masses ($y^n$ < 28.00 kg/m$^3$)*

AASW over the slope exhibits very similar thermohaline characteristics to those of the shelf region in the top 150 m across the three meridional sectors, albeit with a slightly higher temperature (+0.2°C) for the top 50 m (Figure 4d and 4e). The AASW is also slightly less oxygenated than on the shelf region (~330 < O < ~350 $\mu$mol/L from east to west) (Figure 4f).

The ASC is recognisable along the shelf break, by a thick (> 197 m) layer of AASW with mid-range temperatures (-1.77 < $\theta$ < -1.38 °C) and variable salinities (Figure 5). It is most prominently observed between 68°E to 70.5°E where the ASC is wider, covering a broader latitudinal range.

#### *4.2.2 Intermediate water masses (28.00 < $y^n$ < 28.27 kg/m$^3$)*

The ASC is also evident in the middle density layer. A thick (197 < T < 591 m) layer of CDW is found along the entire slope with mid-range temperatures (-0.27 < $\theta$ < 0.43 °C) and mid-range salinity (34.74 < S_A < 34.85 g/kg) (Figure 6). This layer is also widest between 68°E to 70.5°E (Figure 6 & Figure 8).

As with the shelf profiles, salinity increases, and oxygen content decreases with depth (Figure 4d–4f). However, while the shelf temperature is mostly uniform from the surface to the sea floor, the mean temperatures on the slope slowly increase with depth from a minimum at 50 m, peaking at ∼600 m.

In the eastern sector at this inflection depth (∼600 m), CDW is warmer (∼0.6°C) and saltier (∼34.85 g/kg). This sector also observes the lowest CDW oxygen content of ∼185 $\mu$mol/L (Figure 4d–4f). Prydz Bay also exhibits a fresh shelf regime as the 28.00 kg/m$^3$ isoneutral has a high angle of intersection with the continental slope (from ∼125 m to ∼300 m) and a flatter density surface than the western sectors (Figure 8e & 8f).

The central sector observes very similar temperature and salinity peaks to the eastern sector, only ∼0.1 °C and ∼0.05 g/kg below the eastern sector (Figure 4d–4f). Here, the 28.00 kg/m$^3$ isoneutral has a lower angle of intersection with the continental slope, tilting from ∼175 m to ∼275 m (Figure 8c & 8d). However, there is a slight shoaling exhibited near the continental slope, creating a slight "V" feature.

In the western sector, the 28.00 kg/m$^3$ isoneutral displays the "V" feature of the ASF, indicative of a dense shelf region (Figure 8a & 8b) (Gill, 1973; Jacobs, 1991; Thompson et al., 2018; Whitworth et al., 1985). There is also a steep drop in mean temperature, paired with an increase in mean oxygen at the inflection depth, but no noticeable change in salinity (Figure 4d–4f). Hence, this sector observes the lowest minimum temperature (∼-0.7°C) and salinity (34.8 g/kg) with the highest oxygen content (275 $\mu$mol/L).

#### *4.2.3 Bottom water masses ($y^n$ > 28.27 kg/m$^3$)*

The bottom density layer on the slope represents mSW. All sectors observe a gradual decrease in temperature and increase in oxygen from 600 to 2000 m depth, while salinity remains fairly constant (Figure 4d–4f). Exported DSW from the shelf region entrains warmer, saltier, offshore water masses, forming warmer (-1.82 < $\theta$ < -0.09 °C) and saltier (34.70 < S_A < 34.84 g/kg) mSW (Figure 7). This mSW signal is also carried westward along the slope from ∼68°E. mSW has a neutral density greater than 28.27 kg/m$^3$, temperature >-1.8°C and <∼-0.7°C, at depths of ∼500 m to 2000 m.

### 4.3 OFFSHORE (bathymetry >2000 m)

#### *4.3.1 Surface water masses ($y^n$ < 28.00 kg/m$^3$)*

Offshore, surface climatology is more homogeneous across the three meridional sectors compared to surface conditions on the shelf and slope (Figure 4a–4c). The greatest variation is exhibited in the eastern sector where the top 150 m has ∼20 $\mu$mol/L lower oxygen content compared to the central and western sectors. In contrast, the western sector has slightly warmer (+ ∼0.3°C) and fresher (- ∼0.05 g/kg) conditions.

#### *4.3.2 Intermediate water masses (28.00 < $y^n$ < 28.27 kg/m$^3$)*

Below 150 m offshore, temperatures and salinity slowly rise, peaking at ∼500 m. This mid-depth peak is warms (0.6 < $\theta$ < 0.8 °C) from east to west, with similar, but more homogenous salinity (34.84 < S_A < 34.87 g/kg) across the three meridional sectors than found on the slope. Oxygen is also more uniform at these mid-range depths compared to the slope region (∼200 < O < ∼210 $\mu$mol/L from east to west) (Figure 4a–4c).

Offshore of Cape Darnley CDW is found spanning the entire study site offshore (150 < depth < 1500 m) as warm (0.2 < $\theta$ < 1.46 °C) and salty (34.71 < S_A < 34.89 g/kg) water (Figure 6). Lower CDW is bounded by the 28.00 and 28.27 kg/m$^3$ isoneutrals, with upper CDW bounded by 27.80 and 28.00 kg/m$^3$ isoneutrals. The upper CDW tongue is observed further south in the western transect, reaching ∼65°S, in comparison to ∼64°S in the central and eastern sectors (Figure 8). This aligns with the warmer mid depth conditions found to the west (Figure 4a).

#### *4.3.3 Bottom water masses ($y^n$ > 28.27 kg/m$^3$)*

Offshore, the bottom density layer is primarily AABW and is found below 1000 m with a neutral density >28.27 kg/m$^3$ (Figure 3a–3c). It can also be identified by a sharp increase in oxygen content at depth, observed in all three sectors (Figure 4a–4c).

Data from this bottom density layer are sparse and do not always reach the seafloor. Therefore, mean thickness calculations are underestimated and unreliable offshore. However, by using bottom of cast data, the temperature (-1.27 < $\theta$ < 1.47°C) and salinity (34.70 < S_A < 35.15 g/kg) range can be identified (see Supp. Figure S4).

There are three shipboard CTD transects that show the upper bound of temperature along the 28.27 kg/m$^3$ isoneutral is ∼0.05°C and salinity upper bound is ∼34.845 g/kg (Figure 8). The transects also show that between the eastern and western transects (both taken in 2021), there is little difference in the thickness of AABW (both ∼1000 m thick). In comparison, AABW in the central transect (taken in 1992) is thicker (∼1400 m thick) than the 2021 transects.

There is also variation in the position of the 28.27 kg/m$^3$ isoneutral on the continental slope. In the western and central transect, it is furthest up the continental slope, reaching a depth of ∼1000 m (Figure 8a – 8d), compared to the eastern sector where this isoneutral intersects with the slope bathymetry at a depth of ∼1700 m (Figure 8e & 8f).

Although AABW is found across all three offshore meridional sectors, its properties differ. Peak oxygen content (∼340 $\mu$mol/L) is found in the western sector, followed by ∼260 $\mu$mol/L in the eastern sector and ∼245 $\mu$mol/L in the central sector (Figure 4c). For both temperature and salinity, a minimum is found in the eastern sector (∼-0.75°C and ∼34.78 g/kg respectively) and a maximum is exhibited in the central sector (∼-0.3°C and ∼34.88 g/kg respectively) with the properties in the western sector falling between these values.

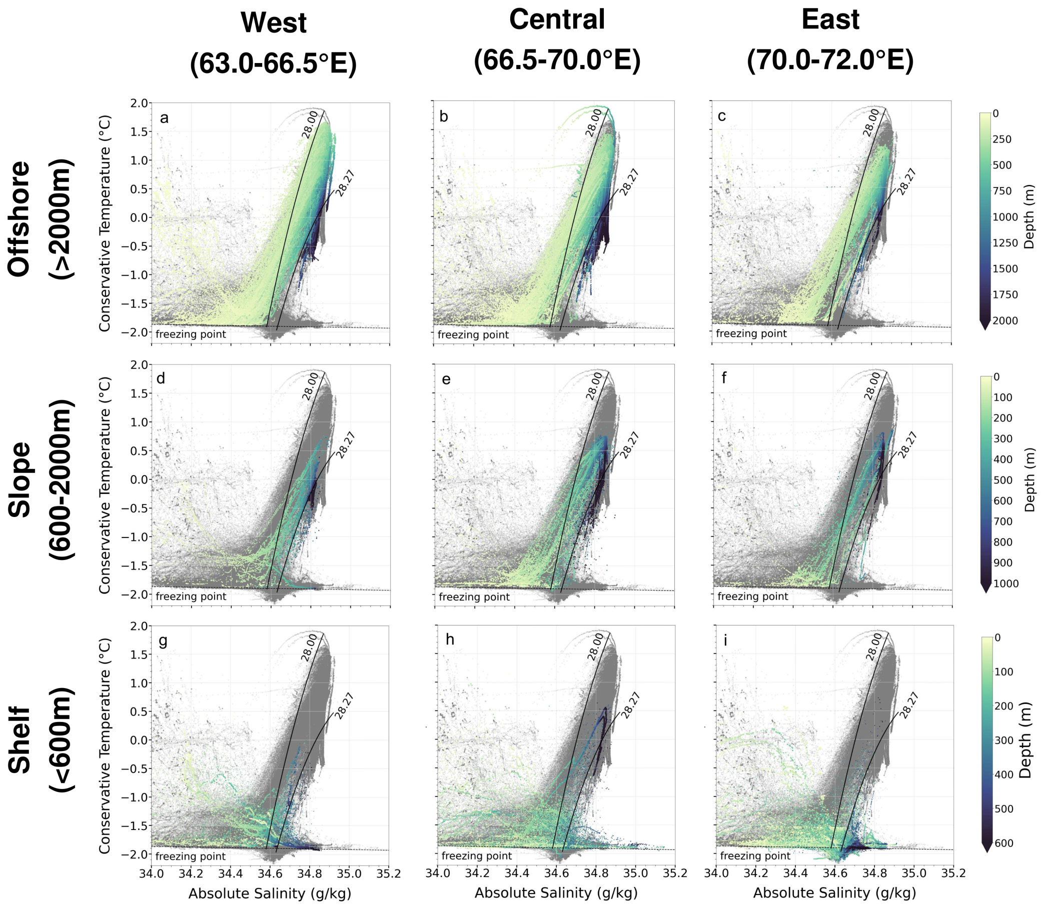


Figure 3: Conservative temperature vs absolute salinity plots for each of the nine sectors in this study, split into east (70-72°E), central (66.5-70°E) & west (63-66.5°E), and shelf (<600 m), slope (600–2000 m) & offshore (>2000 m). The two black lines indicate the 28.00 & 28.27kg/m$^3$ neutral density lines, with points in grey if they fall outside the sector, and coloured by depth if they fall within the sector. The surface freezing point is represented by the black dashed line

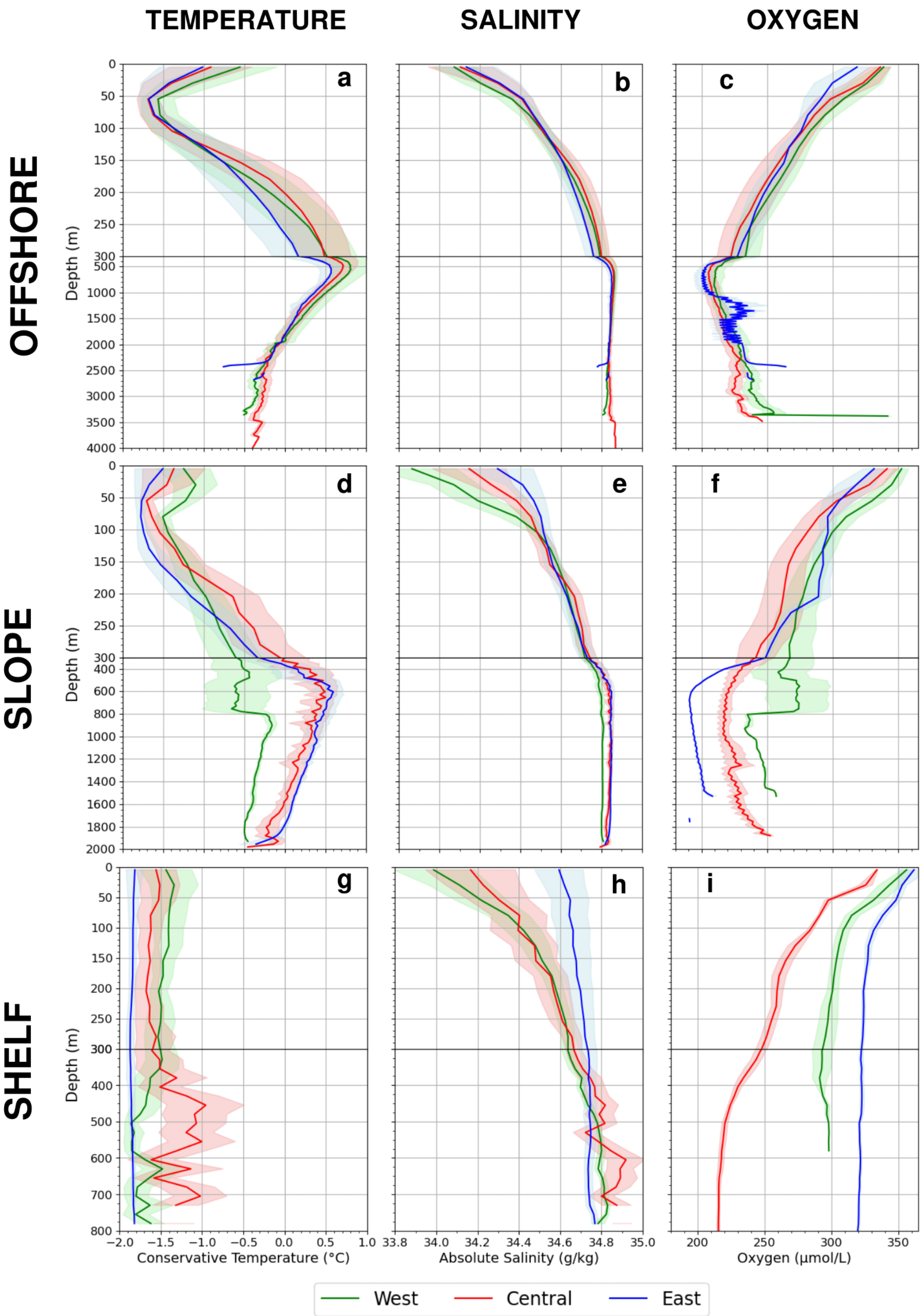


Figure 4: Depth profiles for offshore (a-c), slope (d-f) & shelf (g-i) split into west (green), central (red) and eastern (blue) regions for conservative temperature (a, d g), absolute salinity (b, e, h) and oxygen (c, f, i). The solid lines represent mean value of all data points in that sector every 25 m, with the lighter shaded colours surrounding the solid mean lines representing ±0.5 standard deviations to highlight seasonal & temporal variations.

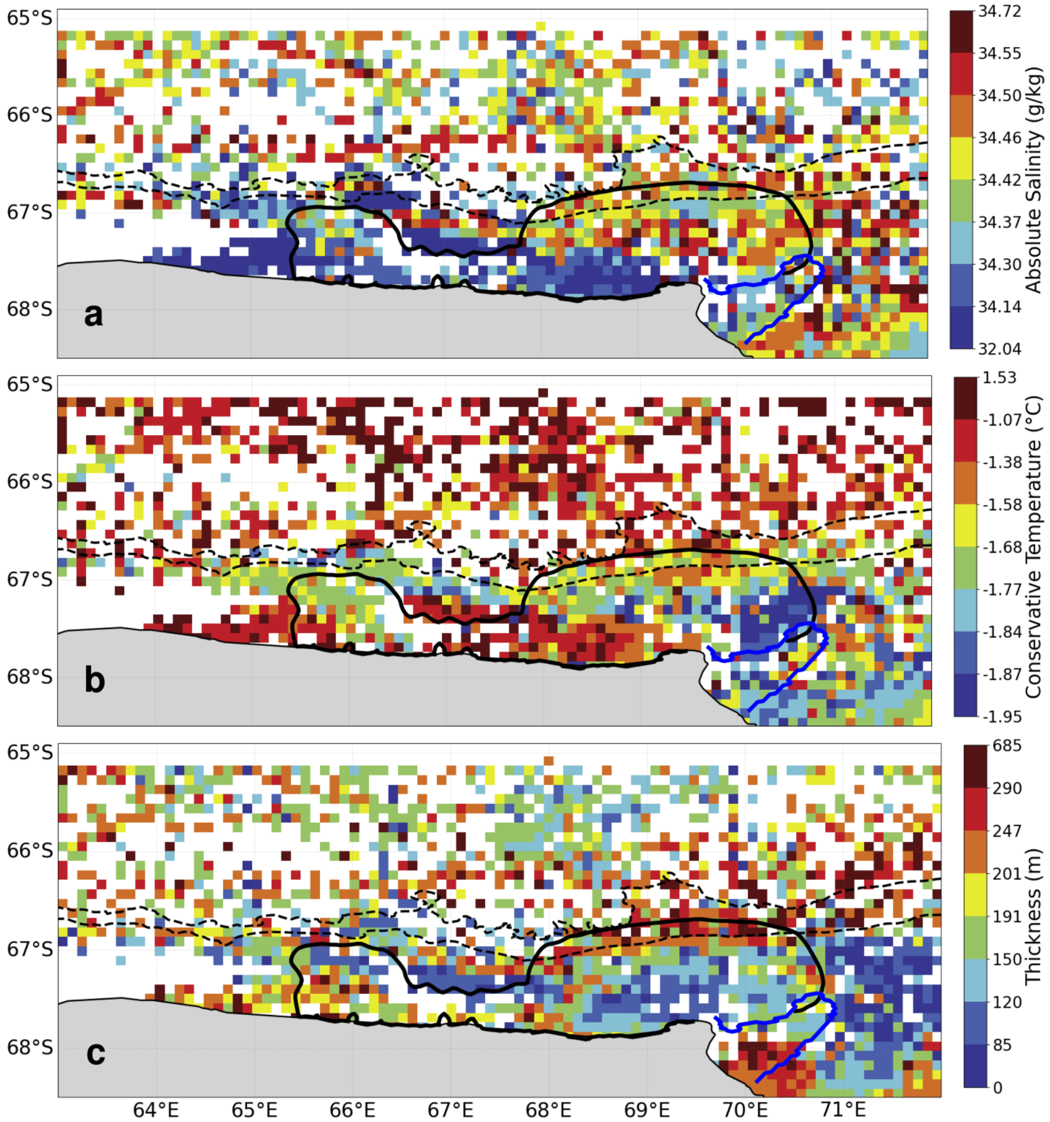


Figure 5: Gridded data of lightest density layer ($y^n < 28.00$ kg/m$^3$) for a) absolute salinity, b) conservative temperature & c) thickness. The black dotted lines represent the 600 m and 2000 m isobaths, the solid black line represents the polynya outline and the solid blue line represents the ice barrier.

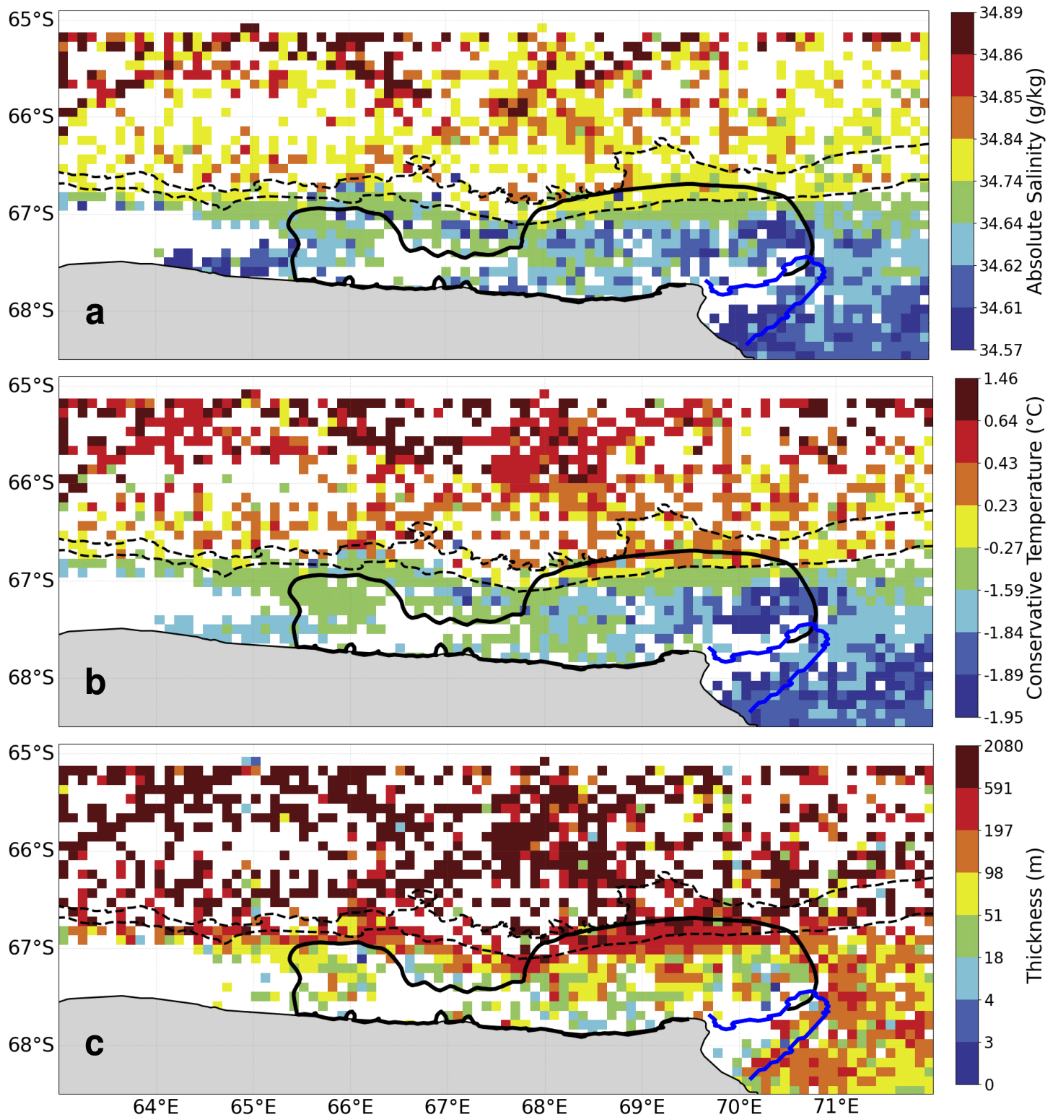


Figure 6: Gridded data of middle density layer ($28.00 < \gamma^n < 28.27$ kg/m$^3$) for a) absolute salinity, b) conservative temperature & c) thickness. The black dotted lines represent the 600 m and 2000 m isobaths, the solid black line represents the polynya outline and the solid blue line represents the ice barrier.

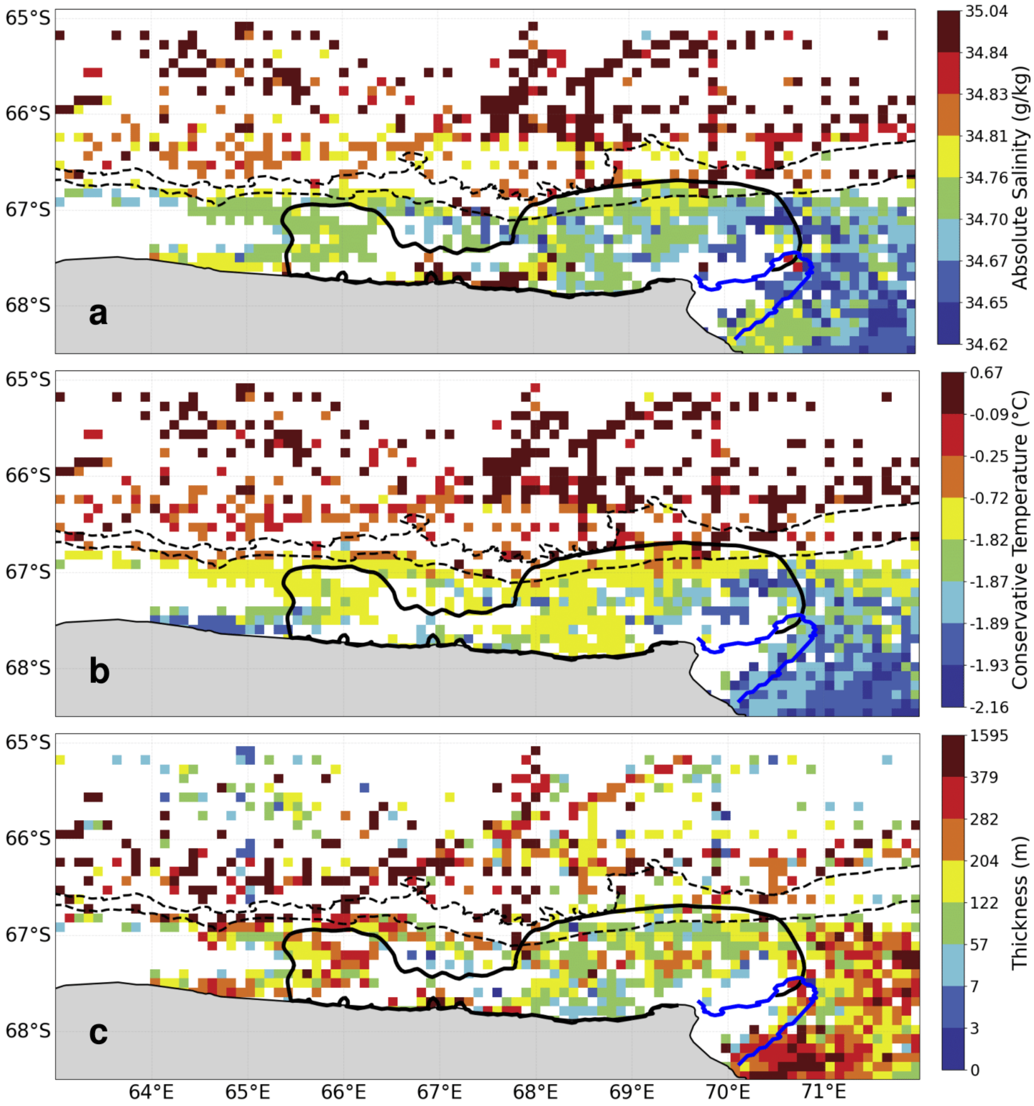


Figure 7: Gridded data of heaviest density layer ($y^n > 28.27$ kg/m$^3$) for a) absolute salinity, b) conservative temperature & c) thickness. The black dotted lines represent the 600 m and 2000 m isobaths, the solid black line represents the polynya outline and the solid blue line represents the ice barrier.

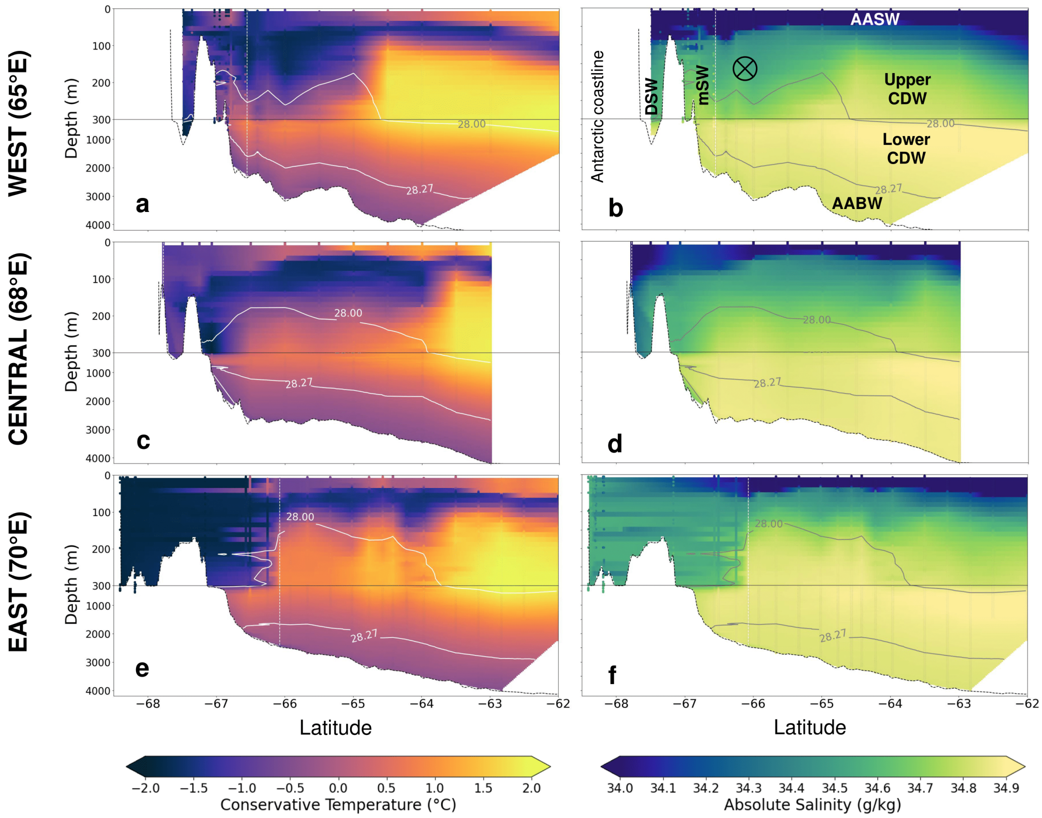


Figure 8: Meridional transects along the west (a & b), central (c & d), & and east (e & f) regions for conservative temperature(a, c & e) and absolute salinity (b, d & f). White/grey solid lines indicate the 28.00 and 28.27 kg/m$^3$ isoneutrals and the black cross circle indicates the approximate location of the Antarctic Slope Current. Interpolated data south of the vertical, dashed white line indicates where the continuous shipboard data for each transect ended and data was pooled from the entire dataset to complete the on shelf transect line. DSW = Dense Shelf Water, mSW = modified Shelf Water, AABW = Antarctic Bottom Water, AASW = Antarctic Surface Water, CDW = Circumpolar Deep Water

# 5 Discussion

## 5.1 Updated water mass classifications

Using this new compilation of oceanographic datasets for the Cape Darnley region, we propose an updated water mass classification for this region (see Table 2). The absolute salinity bounds were determined using the neutral density contours on the TS plot (Figure 3). Furthermore, we assign a lower temperature bound for mCDW of -1.2°C, to separate it from surface waters that fall within the intermediate density class which are following the mixing pathway to DSW (see Section 4.1.2).

Table 2: Updated mass classification for Cape Darnley, East Antarctica (updates highlighted in **bold**), adapted from Orsi et al. (1999); Orsi & Wiederwohl (2009); Portela et al. (2021). Updated temperature and salinity bounds were determined from Figures 2 & 8

| Neutral Density $y^n$ (kg/m$^3$) | Water Mass | Depth Range / Location | Absolute Salinity (g/kg) | Conservative Temperature (°C) |
|---|---|---|---|---|
| $y^n$ <28.00 | AASW | **<2000 m** | **<34.85** | >-1.95 |
| 28.00 <$y^n$ <28.27 | CDW | | **34.85 <S_A <34.90** | |
| | mCDW | | | **>-1.2** |
| - | ISW | **On shelf** | | <-1.95 |
| $y^n$ >28.27 | DSW | | **>34.62** | -1.95 <$\theta$ <-1.85 |
| | mSW | **Slope (600–2000 m)** | | >-1.85 |
| | AABW | **>1000 m** | **34.82 <S_A <34.85** | **<0.05** |

[1] Note: AASW = Antarctic Surface Water; CDW = Circumpolar Deep Water; mCDW = modified CDW; ISW = Ice Shelf Water; DSW = Dense Shelf Water; mSW = modified Shelf Water; AABW: Antarctic Bottom Water

## 5.2 Oceanic processes in the different meridional sectors of the Cape Darnley region

### *5.2.1 Eastern sector*

In the eastern sector, Prydz Bay Gyre observes unique shelf conditions. Here we observe the thinnest, coldest, and saltiest AASW. These attributes arise from the proximity of the Amery Ice Shelf, contributing cold water, and the mixing of saline mCDW that intrudes onto the shelf via the Prydz Bay cyclonic gyre (Portela et al., 2021; G. Williams et al., 2010) where we observe mCDW gradually increases in thickness to the east. The DSW formed from the Prydz Bay polynyas in this region is the coldest ($-2.16 < \theta < -1.82$ °C) and freshest ($34.62 <$ S_A $< 34.76$ g/kg) of the meridional sectors due to the mixing with ISW formed under the Amery Ice Shelf (G. D. Williams et al., 2016). The resultant reduction in density means the DSW in this region does not reach the critical density to sink to the seafloor and become AABW and is the key reason Prydz Bay DSW is not the primary contributor to CDBW (Nunes Vaz & Lennon, 1996; G. D. Williams et al., 2016).

On the slope, a fresh shelf regime is observed. Here AASW is the thickest of the meridional sectors with a deepening of the 28.00 kg/m$^3$ isoneutral (Figure 8e & 8f). The high angle of intersection of this isoneutral with the continental slope indicates the presence of the ASC and the strongest frontal structure, classified as a fresh shelf regime by Thompson et al. (2018) and highlights that there is no/minimal active AABW formation (Meijers et al., 2010). Although the Prydz Bay region does not contribute DSW directly to CDBW formation, the cool, fresh DSW signal is found travelling wetward along the slope with the ASC, and the cool, salty AASW signal from Prydz Bay is found wrapping around the Cape Darnley Ice Barrier, preconditioning the waters in the Cape Darnley Polynya (Figure 9c & 9d) (Nunes Vaz & Lennon, 1996; G. D. Williams et al., 2016; Ohshima et al., 2013).

#### *5.2.2 Central sector*

The central sector is dominated by the Cape Darnley Polynya. At the surface, within the polynya, we found a sharp gradient in water properties across a line from (67.5°S, 68°E) to (67.8°S, 69.2°E), where north-east of this line has colder and saltier properties (Figure 5), indicating that the westward flow of AASW from Prydz Bay has a limited extent. These surface conditions may also indicate that the north-east portion of the polynya is more active, with greater exposure to the atmosphere, reducing surface temperatures and increased brine rejection. This observation is slightly different to sea ice production contours from 2008 published by Ohshima et al. (2013), that indicate the south-east portion of the polynya is the most active. However, our findings could also be supported as sea ice production in this north-east portion could also be aided by the Cape Darnley Ice Barrier (see blue outline in Figure 5), blocking the westward movement of ice, thereby maintaining the polynyas extent.

The combination of the preconditioned AASW and high sea ice production in the north-east portion of the polynya creates DSW that reaches the density required to form CDBW and does not need accumulation time in a shelf basin to achieve critical density (as seen in regions like the Adélie, Ross and Weddell Seas) (G. D. Williams et al., 2010). Some of this DSW likely directly flows onto the slope and downstream before descending Wild Canyon (Ohshima et al., 2013). However, the DSW from this active north-east portion and the less active south-west portion of the polynya in this sector also flows westward into Burton Basin (Figure 9b & 9d). Here we observe the highest salinity (up to 35.15 g/kg) DSW signal (Figures 3h & 7a), that we have coined Burton Basin DSW (Figure 9b & 9d). It must be noted that this dense water (below the 28.27 kg/m$^3$) is not observed in the interpolated transects on the central shelf (Figure 8c & 8d). This is likely a limitation of the method used to produce the shelf transect that introduced interannual/seasonal variability and greater horizontal interpolation, or alternatively the 68°E transect line may not lie along the lowest point of the basin, missing the DSW. Instead, we conclude that salinity peaks in this sector due to its proximity to the largest, most active portion of the polynya paired with preconditioning from Prydz Bay DSW.

The flow of Burton Basin DSW over the continental shelf changes the slope regime. This is highlighted by the shoaling of isoneutrals along the slope, creating a slight "V" shape (Figure 8b). This shoaling also allows for warmer offshore CDW to intrude onto the shelf (as indicated in Figure 6b as water between -1.59 and -0.27°C) also via the Burton Basin. This sector was broadly categorised as a dense shelf regime by Thompson et al. (2018). However, the shape of the isoneutrals sit between those categorised for a fresh and dense shelf regime, therefore we redefine the central sector as a transitional regime. The ASC is visible along the upper slope as a thick layer of warmer AASW (Figure 5). North of Cape Darnley (between 68.8–69.5°E), there is an increase in the width of this current that may be the result of this region being more highly resolved by the dataset, alternatively it may also suggest that the more gradual incline of the slope bathymetry is causing the westward ASC to decelerate and form eddies due to the change in slope gradient. Hence, the ASF here is wider, represented by a more gradual incline of isoneutrals moving offshore compared to the eastern sector (Figure 8c & 8d).

Once the Burton Basin DSW has overflown the continental shelf, it descends down Wild Canyon (Ohshima et al., 2013). On the slope, it transitions into mSW as it mixes with offshore water masses before becoming CDBW at depths of ∼1000 m or greater (Figure 8c & 8d). We found AABW in the central sector is the shallowest and thickest observed across the three sectors. This could be a regional difference caused by variations in DSW production along the Cape Darnley shelf. However, it could also be a temporal difference as this central transect was collected in 1992, while the eastern and western transects were collected in 2021. Thus, the difference in thickness may be related to the freshening and contracting of AABW over 30 years (G. D. Williams et al., 2010; Tamura et al., 2008; Fogwill et al., 2015; Gunn et al., 2023). To better resolve the DSW and AABW spatial formation in the Cape Darnley region, contemporaneous transects across the three sectors would be required to remove temporal and seasonal variations for comparison.

#### *5.2.3 Western sector*

The western sector shelf has similar oceanographic processes to the central sector. Here we found AASW on the shelf is the freshest and warmest, similar to the south-west portion of the polynya within the central sector, as the cold surface water from Prydz Bay appears to have little influence on this shelf sector. Instead, most of the westward flow of water from the eastern sector is found over the shelf break and slope in this western sector (Figure 5). Shelf AASW is thickest over the Nielsen Basin, reaching up to 640 m in this sector. This thick AASW close to the MacRobertson Land ice sheet could explain the small ISW signal observed along the coast (Supp. Figure S3). Beneath the polynya, DSW in this sector is primarily observed within the Nielsen Basin (Figure 7) which we have coined Nielsen Basin DSW. The DSW here is likely a combination of Burton Basin DSW that has flowed westward from the central sector and new DSW formed by the western portion of the polynya. This Nielsen Basin DSW has slightly fresher properties (maximum salinity of 34.85 g/kg) than that in the central sector (Figure 3g), with a different export pathway down the Daly Canyon (Figure 9a & 9d).

From the export of this DSW down the Daly Canyon, we observe a dense slope regime. An increase in slope oxygen and shoaling of the 28.00 kg/m$^3$ isoneutral indicate the presence of mSW on the slope, forming a distinct "V" configuration, indicative of a dense slope regime (Gill, 1973; Jacobs, 1991; Whitworth et al., 1985; Thompson et al., 2018). This "V" formation creates the steepest temperature gradient between the ASC and the offshore CDW tongue that protrudes the furthest south (to 64.5°S) in this sector, which aligns with the southernmost protrusion of the Antarctic Circumpolar Current (Meijers et al., 2010). The shoaling of isoneutrals along the slope also allows for CDW intrusion, which is exhibited as a thicker and warmer layer moving south, up the Nielsen Basin in this western sector (Figure 6b). The onshore mCDW intrusion is increased here due to the reduced sea surface height associated with DSW offshore pulses Morrison et al. (2020).

Offshore, the mSW is transformed into CDBW at depths >1000 m. Although the temperature and salinity properties of CDBW in this western sector sit between the central and eastern sector, oxygen content is ∼70 $\mu$mol/L above the other sectors. This is likely the result of DSW transport from the active central sector combined with DSW formation in the western sector. Thus, we suggest a higher volume of new CDBW is exported via the Nielsen Basin in the western sector compared to the Burton Basin in the central sector.

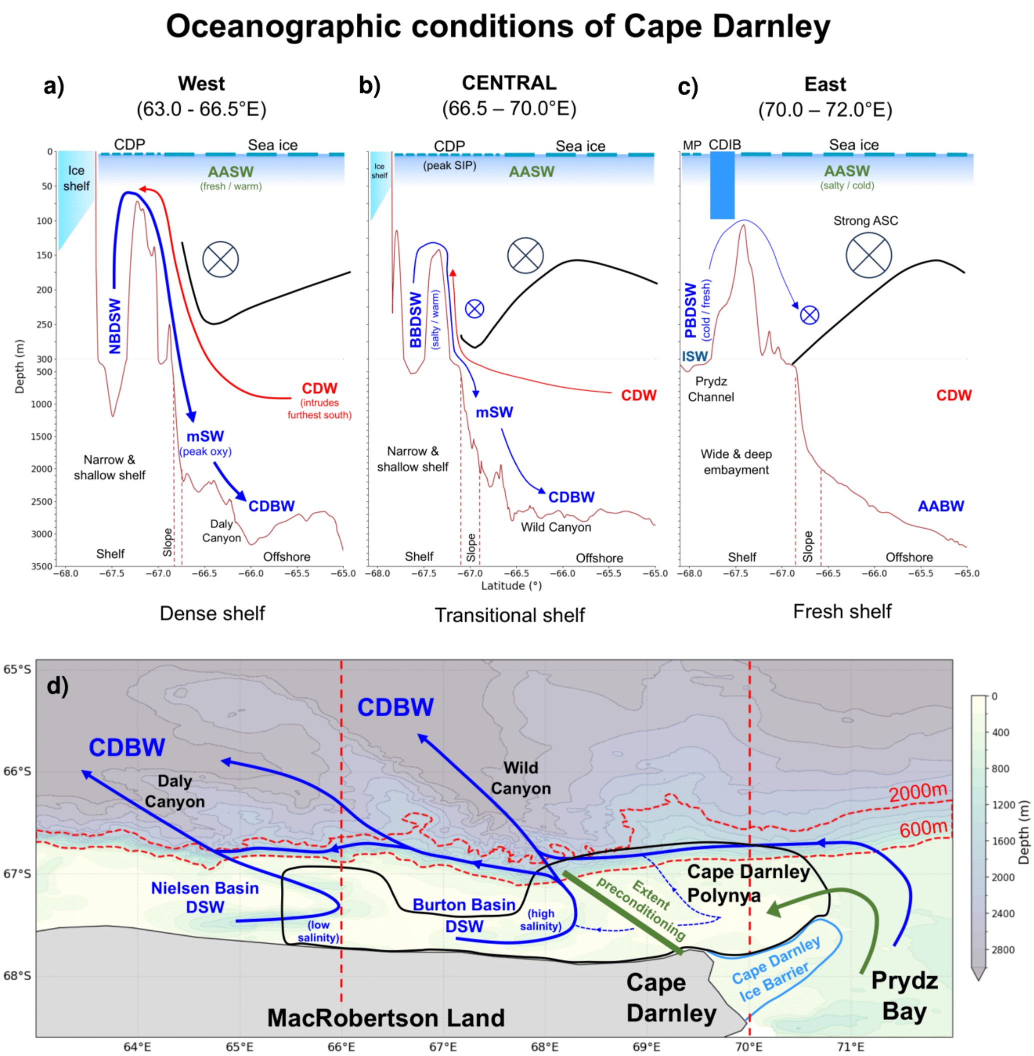


Figure 9: Schematic of Cape Darnley sectors (a - west, b - central, c - east) with bathymetry (brown), 28.00 kg/m$^3$ isoneutral (black), direction of Antarctic Slope Current (ASC) (black cross circle) and direction DSW slope flow (blue cross circle). Plan view (d) shows sectors, isobaths (600 2000 m – horizontal, dashed red lines), longitudinal split (vertical, dashed red lines) Cape Darnley Polynya (CDP - black), Cape Darnley Ice Barrier (CDIB - light blue), transport pathways of Dense Shelf Water (DSW) and Cape Darnley Bottom Water (CDBW) (solid dark blue), proposed DSW pathway of DSW from the north-east portion of the CDP (dashed dark blue), and extent of surface preconditioning from Prydz Bay (green). AASW = Antarctic Surface Water, mSW = modified shelf water, CDW = circumpolar deep water, AABW = Antarctic Bottom Water, PB = Prydz Bay, NB = Nielsen Basin, BB = Burton Basin, CDP = Cape Darnley Polynya, MP = Mackenzie Polynya

#### *5.2.4 Comparison of CDBW characteristics to other AABW formation regions*

The formation of AABW at Cape Darnley (CDBW) is unique compared to the Ross Sea, Weddell Sea and Adélie Land bottom water formation sites as it doesn't have a shelf basin where the DSW can accumulate and densify through the season. Instead we propose that the key mechanism for CDBW formation is the preconditioning of cold, salty surface waters from the eastern sector (Prydz Bay) which flows west on the shelf to ∼68.5°E and facilitates high sea ice formation within the Cape Darnley Polynya. Thus, the DSW formed at Cape Darnley reaches a critical density to overflow the sill, despite the absence of a shelf basin. We identify these conditions produce the highest absolute salinity compared to other AABW formation sites, with a maximum salinity of 35.15 g/kg (0.08 g/kg above that previously recorded 35.07 g/kg in this region; Ohshima et al. (2013)). We identify a high salinity variant exported through the Burton Basin (up to 35.15 g/kg) and down the Wild Canyon, and a low salinity variant exported through the Nielsen Basin (up to 34.85 g/kg) and down the Daly Canyon. More research is required to quantify the volume of export through these two export pathways in the Cape Darnley region. AABW is defined as having a neutral density of 28.27 kg/m$^3$ or greater (Orsi et al., 1999) and using this definition for the presence of bottom water, we propose that the CDBW has the warmest upper temperature boundary at 0.05°C. The main AABW formation mechanisms across the four formation sites are summarised and compared in Table 3.

Table 3: Comparison of four Antarctic Bottom Water formation sites using outcomes from this study and adapted from Budillon et al. (2011); Wang et al. (2012); G. D. Williams et al. (2010); Ohshima et al. (2013); G. D. Williams et al. (2008); Orsi & Wiederwohl (2009); Marsland et al. (2004); Tamura et al. (2008); Silvano et al. (2020); Foldvik et al. (2004); Gordon et al. (2015).

| | **Cape Darnley** | **Adélie** | **Ross** | **Weddell** |
|---|---|---|---|---|
| **Longitude** | ∼69°E | ∼145°E | ∼170°E | ∼60°W |
| **Blocking Ice Barrier** | Yes – Cape Darnley Ice Barrier | Yes – B-9b and Ninnis Glacier Tongue remnant icebergs | Yes – (only Terra Nova Polynya) Drygalski Ice Tongue | No |
| **Preconditioning from upstream** | Yes, Prydz Bay | No | No | No |
| **Large embayment** | No | Yes | Yes | Yes |
| **Shelf depth** | <400 m | <1000 m | <1000 m | <1000 m |
| **Polynya over shelf break** | Yes | No | No | No |
| **Polynya ice production ($km^3$/yr)** | 181 | 180 | 449.2 | 84.6 |
| **ISW impacting DSW** | Minimal | Minimal | Yes | Yes – biggest influence here |
| **High & low salinity DSW variant** | HSSW<br>Wild Canyon<br>LSSW<br>Daly Canyon | HSSW<br>Adélie Depression<br>LSSW<br>Mertz Depression | HSSW<br>Drygalski Trough<br>LSSW<br>Joides Trough | HSSW<br>From south-west<br>LSSW<br>Near Filchner depression & western shelf |
| **Max DSW absolute salinity observation (g/kg)** | 35.15 | 34.9 | 34.9 | 34.87 |
| **Upper conservative temperature bound of AABW (°C)** | <0.05 | <0 | <-0.1 | <-0.8 |
| **Percent contribution to global AABW** | 6–13% | 2–9% | 30–40% | 50–60% |

[1] Note: ISW = Ice Shelf Water; DSW = Dense Shelf Water; HSSW = High Salinity Shelf Water; LSSW = Low Salinity Shelf Water; AABW: Antarctic Bottom Water

### 5.3 Conclusions

Cape Darnley is a major contributor to global AABW, producing 6–13% of the total AABW formation. However it is the least studied AABW formation site due to its relatively recent discovery in 2013. Here we collate 40 years of oceanographic data available for this region and review the physical oceanography. We identified three distinct meridional sectors (east, central, west), with different oceanographic processes that influence the temperature and salinity characteristics of the DSW that is formed from the polynyas in this region. In comparison to other AABW formation sites, Cape Darnley has no large basin for DSW accumulation. Instead the primary driver of CDBW is high levels of sea ice production from the Cape Darnley Polynya and we found the westward movement of surface waters from Prydz Bay provides cold, salty surface waters to the central sector, to approximately 68.5°E, enhancing sea ice production in the north-east portion of the Cape Darnley Polynya.

We found two distinct DSW variants, a high salinity DSW observed in the Burton Basin and a lower salinity DSW in the Nielsen Basin. Smaller volumes of Burton Basin DSW are exported off shelf under a transitional shelf regime down the Wild Canyon, while larger volumes of Nielsen Basin DSW are exported offshore under a dense shelf regime via the Daly Canyon. This high salinity variant is the saltiest DSW (up to 35.15 g/kg) of all the AABW formation sites. The DSW is transformed to mSW and ultimately to CDBW at depths >1000 m and creates the warmest variant of AABW with an upper temperature bound of 0.05°C and an upper salinity bound of 34.845 g/kg. Collecting repeat transects on the shelf and enhancing sensors (e.g. adding oxygen to seal CTDs) will provide vital information to help determine export volumes, sources, and help to resolve slope and shelf processes at a higher resolution.

## Open Research Section

All sources and information about the raw shipboard CTD data can be found in Table 1. The marine mammal data were collected and made freely available by the International MEOP Consortium and the national programs that contribute to it (`http://www.meop.net`). The location and season of all raw data can be observed in Supp. Figure S1. The source code for the plots used in this study and the data product containing the raw data, gridded, and mean data can be found at 10.5281/zenodo.10976304.

**Acknowledgments**

This research was made possible and funded by ARC DP funding and a grant of sea time on the RV Investigator from the CSIRO Marine National Facility to Helen Bostock and Alix Post. The authors acknowledge support from the science team and crew onboard the RV Investigator IN2023_V01 for their support and advise in the early stages of this study. This research was supported by the use of the Australian Research Data Commons (ARDC) Nectar Research Cloud, a collaborative Australian research platform supported by the NCRIS-funded ARDC.

## References

Aoki, S., Ono, K., Hirano, D., & Tamura, T. (2020). Continuous winter oceanic profiling in the cape darnley polynya, east antarctica. *Journal of oceanography*, *76*(5), 365–372.

Bindoff, N., Rintoul, S., & Massom, R. (2000). Bottom water formation and polynyas in adelie land, antarctica. *Papers and proceedings of the Royal Society of Tasmania*, *133*(3), 51–56.

Blanckensee, S. N. (2024). *Siennaneve/cdobs: Cape darnley, east antarctica, antarctic bottom water data collation nc files.* Retrieved from `doi:10.5281/`

zenodo.10976304[Dataset]

Bourreau, L., Pauthenet, E., Le Ster, L., Picard, B., Portela, E., Sallée, J. B., … Labrousse, S. (2023). First description of in situ chlorophyll fluorescence signal within east antarctic coastal polynyas during fall and winter. *Frontiers in Marine Science*, *10*.

Boyer, T. P., Baranova, O. K., Coleman, C., Garcia, H. E., Grodsky, A., Locarnini, R. A., … Zweng, M. M. (2018). *Noaa atlas nesdis 87* (Tech. Rep.). World Ocean Database.

Budillon, G., Castagno, P., Aliani, S., Spezie, G., & Padman, L. (2011). Thermohaline variability and antarctic bottom water formation at the ross sea shelf break. *Deep-sea research. Part I, Oceanographic research papers*, *58*(10), 1002–1018.

Cougnon, E. A., Galton-Fenzi, B. K., Meijers, A. J. S., & Legrésy, B. (2013). Modeling interannual dense shelf water export in the region of the mertz glacier tongue (1992-2007): Modeling interannual dense shelf water. *Journal of geophysical research. Oceans*, *118*(10), 5858–5872.

Darelius, E., Daae, K., Dundas, V., Fer, I., Hellmer, H. H., Janout, M., … Østerhus, S. (2023). Observational evidence for on-shelf heat transport driven by dense water export in the weddell sea. *Nature communications*, *14*(1), 1022–1022.

Dinniman, M. S., Asay-Davis, X. S., Galton-Fenzi, B. K., Holland, P. R., Jenkins, A., & Timmermann, R. (2016). Modeling ice shelf/ocean in antarctica a review. *Oceanography (Washington, D.C.)*, *29*(4), 144–153.

Fogwill, C. J., Phipps, S. J., Turney, C. S. M., & Golledge, N. R. (2015). Sensitivity of the southern ocean to enhanced regional antarctic ice sheet meltwater input. *Earth's future*, *3*(10), 317–329.

Foldvik, A., Gammelsrod, T., Osterhus, S., Fahrbach, E., Rohardt, G., Schroeder, M., … Woodgate, R. A. (2004). Ice shelf water overflow and bottom water formation in the southern weddell sea. *Journal of Geophysical Research*, *109*(C2), C02015–n/a.

Fraser, A. D., Ohshima, K. I., Nihashi, S., Massom, R. A., Tamura, T., Nakata, K., … Willmes, S. (2019). Landfast ice controls on sea-ice production in the cape darnley polynya: A case study. *Remote sensing of environment*, *233*, 111315.

Gao, L., Zu, Y., Guo, G., & Hou, S. (2022). Recent changes and distribution of the newly-formed cape darnley bottom water, east antarctica. *Deep-sea research. Part II, Topical studies in oceanography*, *201*, 105119.

GEBCO Compilation Group. (2023). *Gebco 2023 grid.* Retrieved 14-07-2023, from https://www.gebco.net/data_and_products/gridded_bathymetry_data/gebco_2023/[Dataset]

Gill, A. (1973). Circulation and bottom water production in the weddell sea. *Deep-sea research and oceanographic abstracts*, *20*(2), 111–140.

Gordon, A. L., Huber, B. A., & Busecke, J. (2015). Bottom water export from the western ross sea, 2007 through 2010. *Geophysical research letters*, *42*(13), 5387–5394.

Gunn, K. L., Rintoul, S. R., England, M. H., & Bowen, M. M. (2023). Recent reduced abyssal overturning and ventilation in the australian antarctic basin. *Nature climate change*, *13*(6), 537–544.

Guo, G., Gao, L., Shi, J., & Zu, Y. (2022). Wind-driven seasonal intrusion of modified circumpolar deep water onto the continental shelf in prydz bay, east antarctica. *Journal of geophysical research. Oceans*, *127*(12), n/a.

Herraiz-Borreguero, L., Church, J. A., Allison, I., Pena-Molino, B., Coleman, R., Tomczak, M., & Craven, M. (2016). Basal melt, seasonal water mass transformation, ocean current variability, and deep convection processes along the amery ice shelf calving front, east antarctica. *Journal of geophysical research. Oceans*, *121*(7), 4946–4965.

Herraiz-Borreguero, L., Coleman, R., Allison, I., Rintoul, S. R., Craven, M., &

Williams, G. D. (2015). Circulation of modified circumpolar deep water and basal melt beneath the amery ice shelf, east antarctica. *Journal of geophysical research. Oceans*, *120*(4), 3098–3112.

Huneke, W. G. C., Morrison, A. K., & Hogg, A. M. (2022). Spatial and subannual variability of the antarctic slope current in an eddying ocean–sea ice model. *Journal of physical oceanography*, *52*(3), 347–361.

IOC, SCOR and IAPSO. (2010). *The international thermodynamic equation of seawater – 2010: Calculation and use of thermodynamic properties.* Retrieved 05-07-2022, from `http://www.teos-10.org/`

Jacobs, S. S. (1991). On the nature and significance of the antarctic slope front. *Marine chemistry*, *35*(1), 9–24.

Johnson, G. C. (2008). Quantifying antarctic bottom water and north atlantic deep water volumes. *Journal of Geophysical Research*, *113*(C5), C05027–n/a.

Kitade, Y., Shimada, K., Tamura, T., Williams, G. D., Aoki, S., Fukamachi, Y., ... Ohshima, K. I. (2014). Antarctic bottom water production from the vincennes bay polynya, east antarctica. *Geophysical research letters*, *41*(10), 3528–3534.

Kusahara, K., Hasumi, H., & Tamura, T. (2010). Modeling sea ice production and dense shelf water formation in coastal polynyas around east antarctica. *Journal of Geophysical Research*, *115*(C10), n/a.

Marsland, S. J., Bindoff, N. L., Williams, G. D., & Budd, W. F. (2004). Modeling water mass formation in the mertz glacier polynya and adelie depression, east antarctica. *Journal of Geophysical Research*, *109*(C11), C11003–n/a.

McMahon, C. R., Hindell, M. A., Charrassin, J. B., Coleman, R., Guinet, C., Harcourt, R., ... Ribeiro, N. (2023). Southern ocean pinnipeds provide bathymetric insights on the east antarctic continental shelf. *Communications earth environment*, *4*(1), 266–10.

Meijers, A., Klocker, A., Bindoff, N., Williams, G., & Marsland, S. (2010). The circulation and water masses of the antarctic shelf and continental slope between 30 and 80 e. *Deep-sea research. Part II, Topical studies in oceanography*, *57*(9), 723–737.

MEOP. (2015). *Marine mammals exploring the oceans pole to pole.* Retrieved 15-09-2022, from `https://www.meop.net/index.html[Dataset]`

Mizuta, G., Fukamachi, Y., Simizu, D., Matsumura, Y., Kitade, Y., Hirano, D., ... Ohshima, K. I. (2021). Seasonal evolution of cape darnley bottom water revealed by mooring measurements. *Frontiers in Marine Science*, *8*.

Morrison, A. K., McC. Hogg, A., England, M. H., & Spence, P. (2020). Warm circumpolar deep water transport toward antarctica driven by local dense water export in canyons. *Science advances*, *6*(18), eaav2516–eaav2516.

National Institute of Polar Research. (2009). *Academic databases.* Retrieved 04-12-2023, from `https://scidbase.nipr.ac.jp/modules/metadata/index.php?content_id=259[Dataset]`

Nunes Vaz, R. A., & Lennon, G. W. (1996). Physical oceanography of the prydz bay region of antarctic waters. *Deep-sea research. Part I, Oceanographic research papers*, *43*(5), 603–641.

Ohashi, Y., Yamamoto-Kawai, M., Kusahara, K., Sasaki, K., & Ohshima, K. I. (2022). Age distribution of antarctic bottom water off cape darnley, east antarctica, estimated using chlorofluorocarbon and sulfur hexafluoride. *Scientific reports*, *12*(1), 8462–8462.

Ohshima, K. I., Fukamachi, Y., Ito, M., Nakata, K., Simizu, D., Ono, K., ... Tamura, T. (2022). Dominant frazil ice production in the cape darnley polynya leading to antarctic bottom water formation. *Science advances*, *8*(42), eadc9174–eadc9174.

Ohshima, K. I., Fukamachi, Y., Williams, G. D., Nihashi, S., Roquet, F., Kitade, Y., ... Wakatsuchi, M. (2013). Antarctic bottom water production by intense sea-ice formation in the cape darnley polynya. *Nature geoscience*, *6*(3), 235–240.

Ohshima, K. I., Nihashi, S., & Iwamoto, K. (2016). Global view of sea-ice production in polynyas and its linkage to dense/bottom water formation. *Geoscience Letters*, *3*(1), 1.

Orsi, A. H., Johnson, G. C., & Bullister, J. P. (1999). Circulation, mixing, and production of antarctic bottom water. *Progress in oceanography*, *43*(1), 55–109.

Orsi, A. H., Smethie, W. M., & Bullister, J. L. (2002). On the total input of antarctic waters to the deep ocean; a preliminary estimate from chlorofluorocarbon measurements. *Journal of Geophysical Research*, *107*(C8), 31-1–31-14.

Orsi, A. H., & Wiederwohl, C. L. (2009). A recount of ross sea waters. *Deep-sea research. Part II, Topical studies in oceanography*, *56*(13), 778–795.

Portela, E., Rintoul, S. R., Bestley, S., Herraiz-Borreguero, L., Wijk, E., McMahon, C. R., … Hindell, M. (2021). Seasonal transformation and spatial variability of water masses within mackenzie polynya, prydz bay. *Journal of geophysical research. Oceans*, *126*(12), n/a.

Portela, E., Rintoul, S. R., Herraiz-Borreguero, L., Roquet, F., Bestley, S., Wijk, E., … Hindell, M. A. (2022). Controls on dense shelf water formation in four east antarctic polynyas. *Journal of geophysical research. Oceans*, *127*(12), n/a.

Sea-Bird Scientific. (2023). *Sbe 9plus ctd.* Retrieved 04-12-2023, from `https://www.seabird.com/asset-get.download.jsa?id=54663149001`

Sea-Bird Scientific. (2024). *Sbe 911plus ctd.* Retrieved 04-12-2023, from `https://www.seabird.com/sbe-911plus-ctd/product?id=60761421595`

Shapiro, G. I., Huthnance, J. M., & Ivanov, V. V. (2003). Dense water cascading off the continental shelf. *Journal of Geophysical Research*, *108*(C12), 3390–n/a.

Silvano, A., Foppert, A., & Macdonald, A. M. (2020). Recent recovery of antarctic bottom water formation in the ross sea driven by climate anomalies. *Nature geoscience*, *13*(12), 780–786.

Tamura, T., Ohshima, K. I., Fraser, A. D., & Williams, G. D. (2016). Sea ice production variability in antarctic coastal polynyas. *Journal of geophysical research. Oceans*, *121*(5), 2967–2979.

Tamura, T., Ohshima, K. I., & Nihashi, S. (2008). Mapping of sea ice production for antarctic coastal polynyas: Mapping of sea ice production. *Geophysical research letters*, *35*, n/a.

Thompson, A. F., Stewart, A. L., Spence, P., & Heywood, K. J. (2018). The antarctic slope current in a changing climate. *Reviews of geophysics (1985)*, *56*(4), 741–770.

Wang, Q., Danilov, S., Fahrbach, E., Schröter, J., & Jung, T. (2012). On the impact of wind forcing on the seasonal variability of weddell sea bottom water transport. *Geophysical research letters*, *39*(6), n/a.

Whitworth, T., Orsi, A. H., Kim, S., Nowlin, W. D., & Locarnini, R. A. (1985). Water masses and mixing near the antarctic slope front. In *Ocean, ice, and atmosphere: Interactions at the antarctic continental margin* (pp. 1–27). Washington, D. C: American Geophysical Union.

Williams, G., Nicol, S., Aoki, S., Meijers, A., Bindoff, N., Iijima, Y., … Klocker, A. (2010). Surface oceanography of broke-west, along the antarctic margin of the south-west indian ocean ( 30 − 80 e ). *Deep-sea research. Part II, Topical studies in oceanography*, *57*(9), 738–757.

Williams, G. D., Aoki, S., Jacobs, S. S., Rintoul, S. R., Tamura, T., & Bindoff, N. L. (2010). Antarctic bottom water from the adelie and george v land coast, east antarctica (140-149 degrees e). *Journal of Geophysical Research*, *115*(C4), n/a.

Williams, G. D., Bindoff, N. L., Marsland, S. J., & Rintoul, S. R. (2008). Formation and export of dense shelf water from the adelie depression, east antarctica. *Journal of Geophysical Research*, *113*(C4), C04039–n/a.

Williams, G. D., Herraiz-Borreguero, L., Roquet, F., Tamura, T., Ohshima, K. I., Fukamachi, Y., … Hindell, M. (2016). The suppression of antarctic bottom water formation by melting ice shelves in prydz bay. *Nature communications*, *7*(1), 12577–12577.

*JGR: Oceans*

Supporting Information for

# A review of the oceanography and Antarctic Bottom Water formation offshore Cape Darnley, East Antarctica

Sienna N. Blanckensee[1], David E. Gwyther[1], Ben K. Galton-Fenzi [2], Kathryn L. Gunn [3], Laura Herraiz-Borreguero[4,5], Kay I. Ohshima [6], Esther Portela Rodriguez[7], Alexandra L. Post [8], Helen C. Bostock[1]

[1]School of the Environment, The University of Queensland, Australia
[2]Australian Antarctic Division, Hobart, Tasmania, Australia
[3]School of Ocean and Earth Science, University of Southampton, Southampton, UK
[4]CSIRO Environment, Hobart, Tas, 7004, Australia
[5]Australian Antarctic Partnership Program, Hobart, Tas, 7004, Australia
[6]Institute of Low Temperature Science, Hokkaido University, Japan
[7]Laboratoire d'Oceanographie Physique et Spatiale (LOPS), University Brest, CNRS, IRD, Ifremer, Plouzane, France
[8]Geoscience Australia, Canberra, Australia

## Contents of this file

Figures S1 to S4

## Introduction

In this study we compile 40 years of oceanographic data for Cape Darnley, East Antarctica, to provide the climatological oceanographic conditions, and review the water mass properties in this region and their role in Antarctic Bottom Water formation. Our findings will contribute to planning future observing systems at Cape Darnley, determining the role Cape Darnley Bottom Water plays in our global oceanic and climate systems, and modelling past and future climate scenarios.

This collated dataset was transformed into TEOS-10 standards (i.e. absolute salinity, conservative temperature, and neutral density) for comparison. Further quality control was completed (i.e. >3 standard deviations from mean) and the output of this collation containing the raw data, gridded, and mean data can be found at 10.5281/zenodo.10976304.

These supplementary figures provide additional spatial and temporal information on the data sources and water masses discussed in the associated paper. These also provide visual comparison between different data sources. All processing for these figures is discussed in the associated paper.

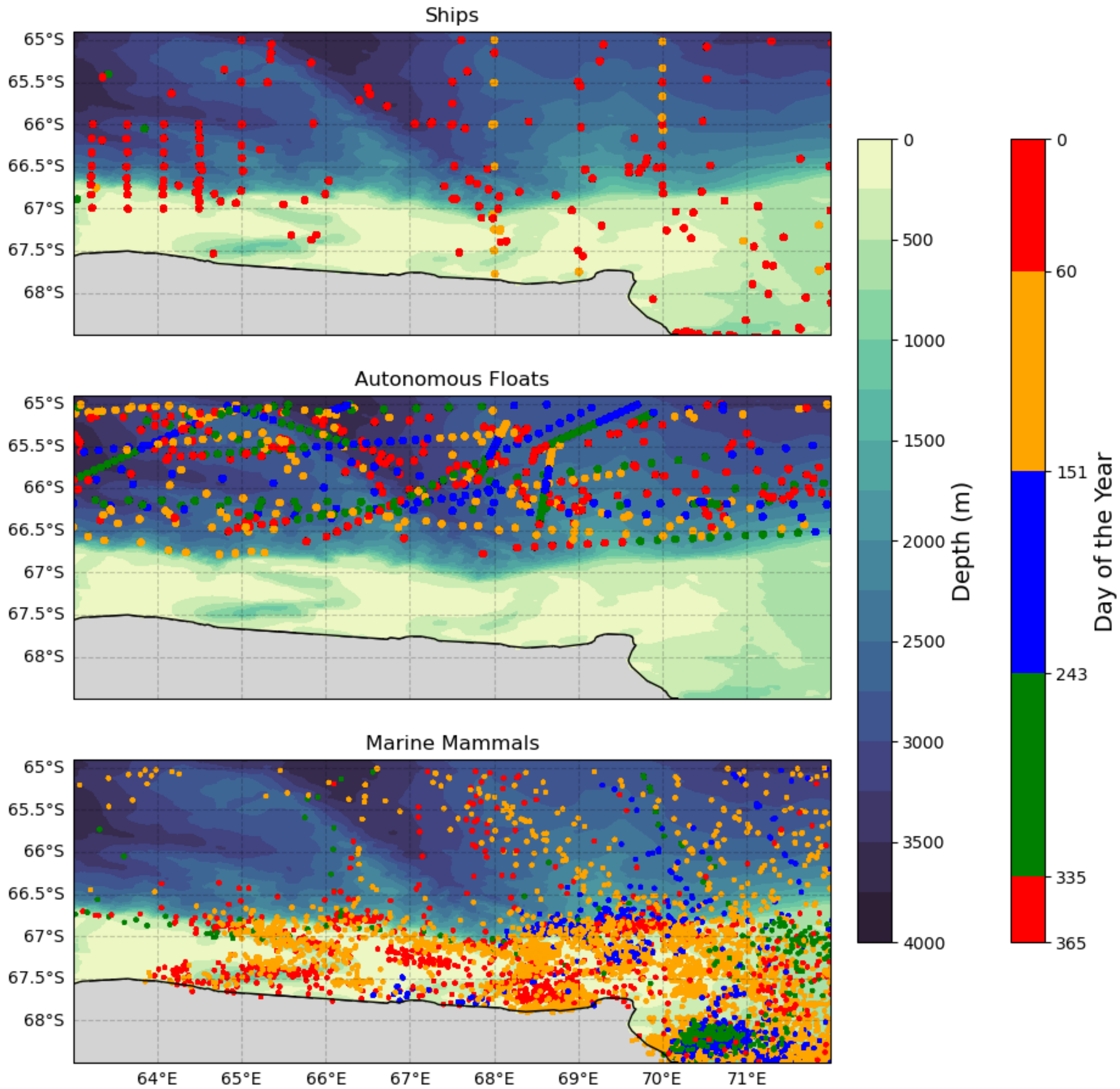


**Figure S1.** The location and austral season of data collected from ships, autonomous floats & seals (marine mammals) where red = summer, orange = autumn, blue = winter & green = spring, with bathymetry contours beneath.

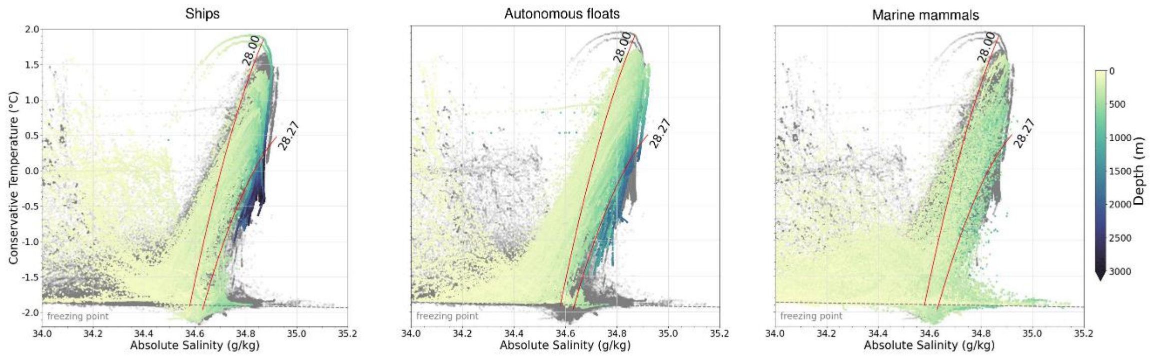


**Figure S2.** Conservative temperature vs absolute salinity plots for each of the three data sources (ships, autonomous floats & seals). The two red lines indicate the 28.00 & 28.27kg/m$^3$ neutral density lines, with points in grey if they are not from the currently plotted data source, and coloured by depth if they are the current data source. The surface freezing point is represented by the grey dashed line.

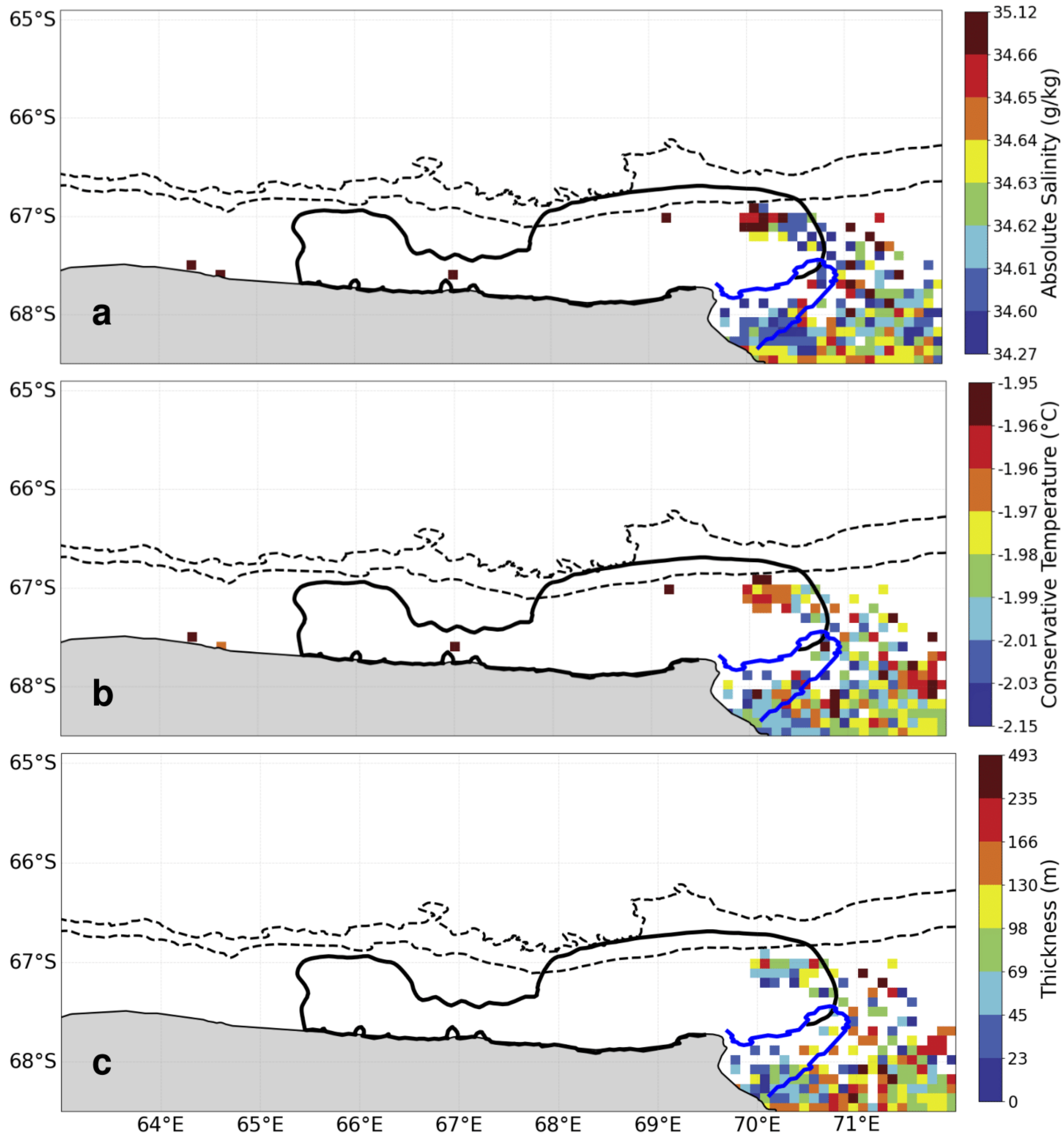


**Figure S3.** Gridded data of Ice Shelf Water (θ < -1.95°C) for a) absolute salinity, b) conservative temperature & c) thickness. The black dotted lines represent the 600m and 2000m isobaths, the solid black line represents the polynya outline, and the solid blue line represents the ice barrier.

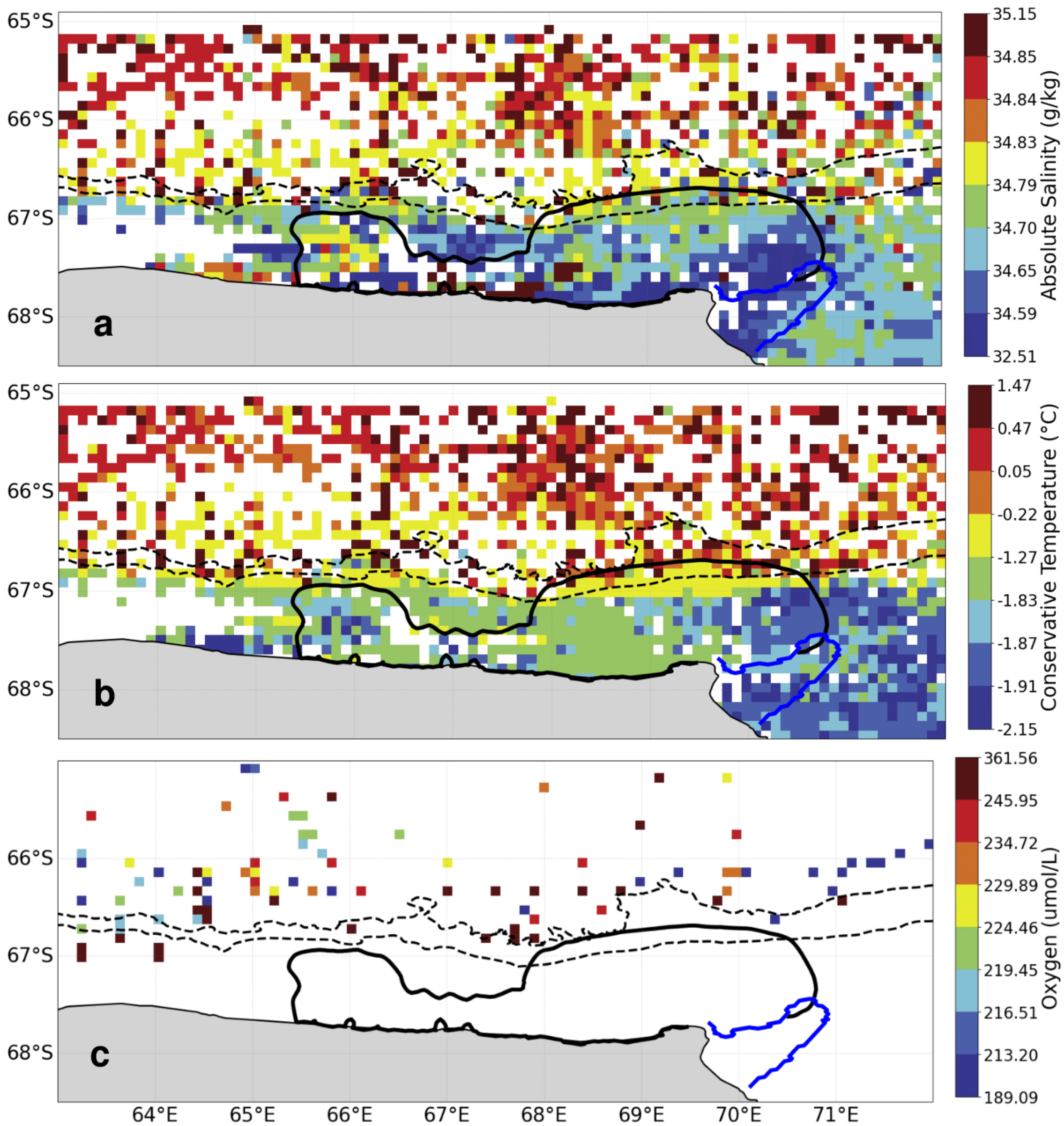


**Figure S4.** Gridded data of bottom of cast for a) absolute salinity, b) conservative temperature & c) oxygen. The black dotted lines represent the 600m and 2000m isobaths, the solid black line represents the polynya outline, and the solid blue line represents the ice barrier.